Neuronal activity–driven oligodendrogenesis in selected brain regions is required for episodic memories

Luendreo P. Barboza[1,2], Benjamin Bessières[1], Omina Nazarzoda[1,3,4], and Cristina M. Alberini[1,5]

[1] Center for Neural Science, New York University, New York

[2] Neuroscience and Physiology, Neuroscience Institute, New York University Langone Medical Center, New York

[3] School of Medicine, University of Virginia, Virginia

[4] School of Natural and Behavioral Sciences, CUNY Brooklyn College, New York

[5] Correspondence to Cristina M. Alberini, Center for Neural Science, 4 Washington Place Room 824, New York University; New York, USA; ca60@nyu.edu

Impact statement: Oligodendrogenesis is required in the anterior cingulate cortex but not in the hippocampus for long-term memory consolidation.

Keywords: episodic memory, oligodendrogenesis, hippocampus, anterior cingulate cortex, rat, mouse

Abstract

The formation of long-term episodic memories requires the activation of molecular mechanisms in several regions of the medial temporal lobe, including the hippocampus and anterior cingulate cortex (ACC). The extent to which these regions engage distinct mechanisms and cell types to support memory formation is not well understood. Recent studies reported that oligodendrogenesis is essential for learning and long-term memory; however, whether these mechanisms are required only in selected brain regions is still unclear. Also still unknown are the temporal kinetics of engagement of learning-induced oligodendrogenesis and whether this oligodendrogenesis occurs in response to neuronal activity. Here we show that in rats and mice, episodic learning rapidly increases the oligodendrogenesis and myelin biogenesis transcripts *olig2*, *myrf*, *mbp*, and *plp1*, as well as oligodendrogenesis, in the ACC but not in the dorsal hippocampus (dHC). Region-specific knockdown and knockout of *Myrf*, a master regulator of oligodendrocyte maturation, revealed that oligodendrogenesis is required for memory formation in the ACC but not the dHC. Chemogenetic neuronal silencing in the ACC showed that neuronal activity is critical for learning-induced oligodendrogenesis. Hence, an activity-dependent increase in oligodendrogenesis in selected brain regions, specifically in the ACC but not dHC, is critical for the formation of episodic memories.

Introduction

Long-term memories are initially fragile but become resilient to disruption through consolidation, a temporally graded process that engages cascades of molecular mechanisms in select brain regions. Episodic memories become consolidated by rapidly recruiting molecular changes in several brain regions, including the hippocampus, medial prefrontal cortex (mPFC), and anterior cingulate cortex (ACC) (Frankland & Bontempi, 2005; Kandel et al., 2014; Squire et al., 2015). Whereas the molecular changes recruited by the hippocampus are needed to continue for days, those recruited in the cortices are persistently required for weeks (Heyward & Sweatt, 2015; Chen et al., 2020), suggesting that there is differential engagement, and therefore distinct biological regulations in different regions underlying memory consolidation and storage. This agrees with the observation that regions of the brain differ in biological composition as a result of their unique cellular populations and regulate distinct molecular pathways in response to learning (Saunders et al., 2018; Chen et al., 2020; Katzman et al., 2021).

Although research in the field of learning and memory has thus far mostly focused on neuronal mechanisms and circuitry, in the last decade it has become clear that long-term memory formation requires the contribution of multiple cell types, including astrocytes (Gerlai et al., 1995; Suzuki et al., 2011; Adamsky & Goshen, 2018), microglia (Yirmiya & Goshen, 2011; Morris et al., 2013), and oligodendrocytes (McKenzie et al., 2014; Xin & Chan, 2020). Recent reports showed that oligodendrogenesis and *de novo* myelination play critical roles in the formation of several types of memory, including motor, spatial, and episodic (McKenzie et al., 2014; Pan et al., 2020; Steadman et al., 2020; Wang et al., 2020) as well as in sensory enrichment (Hughes et al., 2018). These studies examined the role of oligodendrocytes by assessing brain-wide oligodendrogenesis, however, several questions remain to be addressed. First, are distinct brain regions differentially engaging oligodendrocytes mechanisms in learning and memory? Second, what is the fine temporal engagement of learning-induced oligodendrogenesis? And, finally, does this oligodendrogenesis require neuronal activation?

Steadman et al. (2020) reported that the acquisition of spatial memory in mice is accompanied by an increase in oligodendrocyte precursor cells (OPCs) proliferation and/or differentiation mechanisms in

the ACC, mPFC, and corpus callosum/cingulum (CC/Cg), but not in the hippocampus, suggesting that these regions may differentially engage oligodendrogenesis in memory formation. Yet, whether this is the case remains to be tested. In addition, using brain-wide conditional genetic knockout of myelin regulatory factor (Myrf, a transcription factor required for oligodendrogenesis), the same authors provided evidence that oligodendrogenesis and *de novo* myelination are required for long-term memory formation and for learning-induced ripple-spindle coupling between the hippocampus and ACC, a cross-region synchronization believed to contribute to memory consolidation. Their temporal assessment for the critical role of oligodendrogenesis revealed that global Myrf knockout during learning or the initial phase of memory consolidation disrupts both recent (tested 1 day later) and remote spatial memories (tested 28 days later) (Steadman et al., 2020), whereas Myrf knockout 25 days after training had no effect on memory, leading to the conclusion that spatial learning and/or consolidation, but not remote memory storage, requires oligodendrogenesis. Pan et al. (2020) obtained a different result using another hippocampus-dependent task in mice, contextual fear conditioning. They found that global knockout of *Myrf* prior to learning impairs remote memory (tested 30 days after training) but not recent memory (tested 1 day after training). Hence, while the effect of oligodendrogenesis on recent hippocampus-dependent memories is still under debate, both studies concluded that experience-dependent changes in myelination are required for long-term memory formation. Notably, the contribution of oligodendrocyte mechanisms during acquisition remains to be defined. Finally, while previous work showed that neuronal activity generally promotes oligodendrogenesis and adaptive myelination (Gibson et al., 2014; Baraban et al., 2016) whether the learning-induced oligodendrogenesis requires neuronal activity remains to be established.

To address these questions, we employed inhibitory avoidance (IA), an episodic memory paradigm, in rats and mice. We found that oligodendrogenesis in the ACC, but not dorsal hippocampus (dHC), is rapidly induced and required for memory consolidation, whereas it is dispensable for acquisition and storage of the memory. We also observed that learning-induced oligodendrogenesis in the ACC is dependent upon neuronal activity.

Results

Episodic learning rapidly increases oligodendrocyte-specific mRNAs in the ACC but not dHC in rats

To assess whether episodic learning induces oligodendrocyte-specific changes in the dHC and ACC of rats, we employed IA, a learning paradigm that results in long-term memory formation after a single-context-footshock association (Gold, 1986). We performed a time-course analysis of transcripts typically expressed during oligodendrocyte differentiation and myelin biogenesis using reverse transcription–quantitative polymerase chain reaction (RT–qPCR) on samples collected one hour, one day, and seven days following training (Fig. 1A). We analyzed expression of *myrf*, oligodendrocyte transcription factor 2 (*olig2*), ectonucleotide pyrophosphatase 6 (*enpp6*), myelin basic protein (*mbp*), proteolipid protein 1 (*plp1*), and myelin associated glycoprotein (*mag*). *Olig2* is required for terminal differentiation of OPCs and indirectly induces the transcription of *myrf*, a master regulator of myelin biogenesis (Bujalka et al., 2013; Emery, 2013). MYRF protein binds to the promoter regions of myelin-associated genes and regulates the transcription of *mbp*, *plp1*, and *mag* (Bujalka et al., 2013). Together, the proteins MAG, PLP1, and MBP ensure proper myelin biogenesis, wrapping, compaction, and function (Sherman & Brophy, 2005; Simons & Nave, 2015). ENPP6 is a choline phosphodiesterase involved in lipid metabolism and myelin biogenesis (Morita et al., 2016).

We first confirmed that trained rats exhibited brain activation by assessing the expression of the immediate-early gene *arc* (Bramham et al., 2010; Shepherd & Bear, 2011; Okuno et al., 2012), and observed that expression was increased at one hour after training and had returned to baseline levels at one and seven days after training (Fig. 1B). We found that training led to a rapid and significant increase in the levels of *olig2*, *myrf*, *mbp*, and *plp1* mRNAs in the ACC (Fig. 1C) at 1 hour after training relative to untrained (UT) rats, which remained in the homecage and unpaired control (UP) rats that underwent context and shock exposure in an unassociated fashion. All mRNA transcripts returned to baseline levels at one day and seven days after training. Furthermore, no significant changes in oligodendrocyte-specific

transcripts were detected in the UP group relative to the UT control group, indicating that the mRNA changes observed in trained rats were due to associative learning and not to novel context or shock presentation.

Expression of *olig2*, *myrf*, *plp1*, *mag*, and *mbp* in the dHC over the same time course did not change (Fig. 1D), although a significant increase in enpp6 was detected at 1 hour and persisted at 1 day and 7 days after training. Collectively these data led us to infer that a rapid increase of oligodendrocyte differentiation transcripts following IA learning takes place in the ACC but not dHC, suggesting that there is an ACC-specific activation of oligodendrogenesis and *de novo* myelination following learning.

To determine whether the changes in mRNA expression were reproduced at the protein level, we used western blots to analyze levels of OLIG2, MBP and MAG and also added the axonal membrane protein CASPR (Einheber et al., 1997). Learning led to a significant increase in OLIG2 and CASPR one day after learning, but no changes in MAG and MBP (Fig.1 E–H). We observed no differences in the UP mice compared to the untrained mice, suggesting that the significant increase in OLIG2 was linked to associative learning. We then visualized and quantified the increase in OLIG2 protein in the ACC by performing immunohistochemical staining (Fig. 1I). Quantification of the fluorescence intensity of all OLIG2-positive nuclei in the ACC of trained and untrained mice showed that training significantly increased the amount of OLIG2 in nuclei, but not the number of OLIG2-positive cells normalized to the quantified area. Together, these data indicate that learning leads to rapid increase of oligodendrogenesis and *de novo* myelin synthesis in the ACC but not in the dHC.

Training increases OPC proliferation and oligodendrogenesis in the ACC but not dHC of mice

The induction of *myrf* and *OLIG2* in the ACC but not the dHC of rats following training (Fig. 1) suggests that there is a differential increase in oligodendrogenesis in the ACC. To test this hypothesis, we quantified the rate of dividing oligodendrocytes in the ACC and dHC of mice. We injected the thymidine analog 5-ethynyl-2'-deoxyuridine (EdU) into mice one hour before IA training to label dividing cells and euthanized the animals one day later, when our previous experiments had shown a significant training-

induced increase in OLIG2 protein levels (Fig. 1E, G). We measured the number of proliferating OPCs by counting cells co-stained with fluorescently labeled EdU and antibodies to platelet-derived growth factor receptor alpha (PDGFRα), a marker of OPCs (Rivers et al., 2008). We quantified newly differentiated oligodendrocytes by visualizing cells labelled with EdU and positive for immunostaining with antibodies to OLIG2, a marker of oligodendrocytes at all stages of maturation as well as adenomatous polyposis coli clone CC-1 (CC1), a marker of mature oligodendrocytes (McKenzie et al., 2014).

OPC proliferation and oligodendrocyte differentiation significantly increased in the ACC after IA training (Fig. 2A); however, training did not appear to affect oligodendrocyte differentiation or proliferation in the dHC (Fig. 2B) nor in the hippocampal subregions DG, CA1, CA2, and CA3 (supplementary data Fig. 1). We concluded that oligodendrogenesis is differentially upregulated in the ACC but not the dHC one day after episodic learning.

Myrf knockout disrupts memory formation

Next, we asked whether oligodendrogenesis is required for IA memory formation in mice. We employed a conditional knockout mouse model in which *myrf* is globally deleted in OPCs. Because MYRF is a transcription factor required for oligodendrocyte differentiation, its deletion in OPCs impairs oligodendrogenesis, and therefore new myelin formation, while leaving existing myelin unaffected(McKenzie et al., 2014). We tested the effect of *myrf* knockout in OPCs on long-term memory using a double transgenic mouse line carrying a tamoxifen (TAM)-inducible CreER^{T2} expressed under the OPC-specific promoter *Pdgfrα* and a floxed *myrf* gene (Pdgfra-CreER^{T2} × Myrf$^{floxed/floxed}$; hereafter, P-Myrf$^{floxed/floxed}$). Injections of TAM in the P-Myrf$^{floxed/floxed}$ mice lead to the deletion of *Myrf* from OPCs, thereby preventing their differentiation and thus impairing oligodendrogenesis and the production of new myelin globally (McKenzie et al., 2014). We used Pdgfra-CreER^{T2}-Myrf$^{+/+}$ (P-Myrf$^{+/+}$) wild-type littermates as controls.

To confirm the effect of *myrf* deletion in OPCs on oligodendrocyte differentiation in the brain, TAM-treated P-Myrf$^{floxed/floxed}$ and P-Myrf$^{+/+}$ mice received an injection of EdU one hour before IA training to label proliferating cells and were perfused one day later. Oligodendrogenesis was significantly inhibited in the ACC in P-Myrf$^{floxed/floxed}$ mice, as demonstrated by the significant reduction in the number of cells that were positive for EdU, OLIG2, and CC1 in P-Myrf$^{floxed/floxed}$ mice compared to P-Myrf$^{+/+}$ littermate controls (Fig. 3A).

To test the effect of *Myrf* knockout on memory formation, TAM was administered to Myrf$^{floxed/floxed}$ and P-Myrf$^{+/+}$ mice seven days before IA training, and the mice were tested at 1, 7, and 28 days after training. P-Myrf$^{floxed/floxed}$ mice exhibited significant memory reduction at all time points compared to P-Myrf$^{+/+}$ controls (Fig. 3B). To exclude the potential effects of multiple testing, a second experiment was conducted in which P-Myrf$^{floxed/floxed}$ and P-Myrf$^{+/+}$ littermates were tested only at 28 days after training, and we again observed significant impairment in memory retention (Fig. 3C). We concluded that brain-wide oligodendrogenesis is required for long-term memory formation and that inhibiting oligodendrogenesis before training impairs memory retention at both recent and remote time points post-training.

To determine whether oligodendrogenesis contributes to the persistence or storage of memory, we administered TAM to P-Myrf$^{floxed/floxed}$ and P-Myrf$^{+/+}$ mice 14 days after training, when the consolidation process has significantly advanced (Bambah-Mukku et al., 2014; Squire et al., 2015). Memory retention was tested 14 days after knockout, corresponding to 28 days after training, as well as at 36 days and 56 days after training. No difference was detected between groups (Fig. 3D), indicating that oligodendrogenesis is not required for the persistence, retrieval, or storage of long-term memory.

Finally, to determine whether mechanisms involving oligodendrogenesis play a role in the formation of non-aversive episodic memories, P-Myrf$^{floxed/floxed}$ and P-Myrf$^{+/+}$ littermates were injected with TAM seven days before being trained in novel object location (nOL), a hippocampus-dependent learning paradigm (Mumby et al., 2002; Weible et al., 2009; Pezze et al., 2016) P-Myrf$^{floxed/floxed}$ mice showed a

187 significant nOL memory impairment compared to P-Myrf$^{+/+}$ littermates (Fig. 3E) when tested four hours
188 after training.
189 Thus, *Myrf*-dependent oligodendrogenesis is also required for the formation of non-aversive
190 hippocampus-dependent memories.
191 To exclude that the memory impairments we observed were due to other behavioral responses
192 such as heightened anxiety-like responses or locomotor impairments, we tested P-Myrf$^{floxed/floxed}$ and P-
193 Myrf$^{+/+}$ littermates in open field behavior. Time spent in the center of an open field arena and the distance
194 and velocity traveled in the arena are putative measures of anxiety and locomotion abilities, respectively.
195 No significant differences in anxiety-like and locomotor responses were detected; the time spent in the
196 center and the distance and mean velocity traveled were similar between P-Myrf$^{floxed/floxed}$ and P-Myrf$^{+/+}$
197 littermates (Fig. 3F). Collectively, these results indicate that oligodendrogenesis is required for the
198 formation of long-term hippocampus-dependent memories.
199
200 ***Myrf* knockdown in the ACC but not the dHC of rats impairs memory consolidation but not**
201 **learning**
202 In order to investigate whether oligodendrogenesis is differentially implicated in distinct brain
203 regions and memory processes, we employed a *Myrf* knockdown strategy. Because the P-Myrf$^{floxed/floxed}$
204 global knockout approach used previously affects other tissues and organs where *Myrf* is expressed in
205 addition to the central nervous system, such as the gastrointestinal tract and kidney, employing a region-
206 targeted approach also addresses possible off-target effects of Pdgfrα-driven global *Myrf* deletion. We
207 achieved region-specific and temporally restricted *Myrf* knockdown by using stereotactic injections to
208 deliver an antisense oligodeoxynucleotide (ASO-ODN) specific against *Myrf* (Myrf-ASO), and, as a
209 control, a related scrambled sequence (Myrf-SCR). We injected the ODNs bilaterally into the brain region
210 of interest at various times before and after training.
211 The temporally limited effect of the ODN knockdown approach offers the opportunity to dissect
212 the temporal dynamics of the requirement of specific mRNA translations, in addition to allowing the

definition of anatomical requirements (Taubenfeld et al., 2001; Garcia-Osta et al., 2006; Chen et al., 2011) Hence, we used the Myrf-ASO approach to examine whether learning-induced expression of *Myrf* is required in the ACC for memory acquisition or consolidation.

To verify knockdown of *myrf*, Myrf-ASO and Myrf-SCR were injected bilaterally 15 minutes before training, and *myrf* mRNA levels were measured in the ACC one hour after training, when there is a significant learning-dependent increase in *myrf* expression (Fig. 1C). Rats treated with Myrf-ASO had significantly lower *myrf* mRNA levels compared to those treated with Myrf-SCR (Fig. 4A). Rats injected with Myrf-ASO exhibited no significant differences in MBP protein expression in the ACC one day after training, suggesting that Myrf-ASO treatment does not lead to demyelination (Fig. 4B).

In order to test whether MYRF is required for learning, we bilaterally injected Myrf-ASO or Myrf-SCR into the ACC 15 minutes before training and tested the effect 1 hour after training. We detected no differences in memory between the two groups (Fig. 4C), indicating that MYRF is dispensable in the ACC for learning and short-term IA memory. To test whether MYRF is required for memory consolidation, bilateral injections of Myrf-ASO or Myrf-SCR were administered in the ACC 15 minutes before and six hours after training, then memory was tested one day after training. Rats injected with Myrf-ASO exhibited significant memory impairment one day after training compared to rats that had received Myrf-SCR injections (Fig. 4D), and the impairment persisted at 28 days after training (Fig. 4D). A reminder shock given one day after the remote memory test was unable to reinstate memory, indicating that the memory impairment was not due to a suppressed memory response but likely resulted from disrupted memory consolidation. Furthermore, retraining one day later of rats who had been injected with Myrf-ASO resulted in a long-lasting memory, thereby excluding the possibility that they had experienced memory loss due to damage to the ACC caused by surgery or injections.

By contrast, when Myrf-ASO was injected bilaterally into the dHC 15 minutes before and six hours after IA training, we observed no effect on memory retention; memories of the two treatment groups were similar at one day and 28 days after training (Fig. 4E). The lower level of retention in the dHC relative to the ACC with stereotactic injections is typically observed. Thus, we concluded that *Myrf*-

dependent oligodendrogenesis in the ACC is critical for the consolidation but not the acquisition of IA and is not required in the dHC.

Oligodendrogenesis in the mouse ACC is required for memory formation

Studies published thus far on the role of oligodendrogenesis in memory formation have reported that brain-wide disruption of oligodendrogenesis impairs motor learning, spatial memory, and remote contextual fear memory in mice (McKenzie et al., 2014; Pan et al., 2020; Steadman et al., 2020). Our data in rats indicated that MYRF-induced oligodendrogenesis is essential for memory consolidation in the ACC but not the dHC. To investigate region-specific roles of oligodendrogenesis in memory formation in the mouse brain, we bilaterally injected an adeno-associated viral vector expressing CreER^{T2} driven by the *Mbp* promoter (AAV-Mbp-CreER^{T2}) in Myrf$^{+\backslash+}$ and Myrf$^{flox\backslash flox}$ mice to knock out *Myrf* selectively in either ACC or dHC under the regulation of TAM. After two weeks to allow for viral expression, intraperitoneal injections of TAM were administered four times, once every other day, then mice underwent IA training (Fig. 5A). Diffusion of Chicago blue dye indicated that material injected into the ACC remained mostly confined there (Fig. 5B). Compared to Myrf$^{+\backslash+}$ littermates, Myrf$^{flox\backslash flox}$ mice injected with AAV-Mbp-CreER^{T2} showed a significant decrease in oligodendrogenesis in the ACC (Fig. 5C) one day after training, confirming that the viral injection led to *Myrf* knockout.

To determine the role of oligodendrogenesis in the ACC on behavioral responses, Myrf$^{+\backslash+}$ and Myrf$^{flox\backslash flox}$ littermates were treated with the same viral and TAM injection protocol as above but tested for memory retention at one day and seven days after training. Compared to Myrf$^{+\backslash+}$ littermates, Myrf$^{flox\backslash flox}$ mice showed a significant memory impairment at both time points after training.

To test whether ACC-specific oligodendrogenesis is required for learning and short-term memory, another cohort of Myrf$^{+\backslash+}$ mice and Myrf$^{flox\backslash flox}$ littermates were treated with the same viral injection and TAM protocol but tested at one hour after IA training. No differences between groups were observed (Fig. 5D, E), leading us to conclude that oligodendrogenesis in the ACC is necessary for

memory consolidation but dispensable for memory acquisition and short-term memory in mice, just as in rats.

To test whether oligodendrogenesis is required for memory formation in the hippocampus, AAV-Mbp-CreER^{T2} was bilaterally injected into the dHC of Myrf$^{+\backslash+}$ and Myrf$^{flox\backslash flox}$ littermates using the protocol described above. No differences in memory retention were observed at one day or seven days post-training compared to control groups (Fig. 5F), leading us to conclude that oligodendrogenesis is required in the ACC for memory consolidation but not for learning or short-term memory. By contrast, oligodendrogenesis is dispensable in the dHC for the formation of hippocampus-dependent memories.

DREADD-mediated neuronal inhibition impairs learning-induced oligodendrogenesis

Neuronal activity can drive oligodendrogenesis and adaptive myelination (Gibson et al., 2014) however, it was not known whether neuronal activity is required to induce learning-dependent oligodendrogenesis. To address this question, we employed the adeno-associated virus 8 (AAV8) expressing the Gi-coupled Designer Receptor Exclusively Activated by Designer Drugs (DREADD) hM4Di under the control of the human synapsin promoter to target expression to neurons (AAV-hSn-hM4D(Gi)-mCherry). We injected AAV-hSyn-hM4D(Gi)-mCherry bilaterally in the ACC and after two weeks to allow for viral expression, we administered its DREADD ligand compound 21 (C21) intraperitoneally (IP) one hour before IA training to transiently silence neuronal activity in the ACC (Jendryka et al., 2019; Tran et al., 2020; Luo et al., 2021). In addition to hM4Di, the AAV-hSyn-hM4D(Gi)-mCherry viral construct expresses the fluorescent protein mCherry in neurons. Fluorescence was assessed by confocal microscopy two weeks after viral infection and found to be mostly confined to the ACC (Fig. 6A). The mice were tested one day after training. Treatment with C21 significantly impaired memory retention compared to vehicle injection (Fig. 6B), suggesting that neuronal activity in the ACC is required for memory formation.

To determine whether blocking neuronal activity in the ACC affected learning-dependent oligodendrogenesis, AAV-hSyn-hM4D(Gi)-mCherry was bilaterally injected into the ACC and fourteen

days later the mice were injected with either C21 or vehicle in combination with EdU two hours before receiving IA training. The mice were perfused one day after training and oligodendrogenesis was assessed by performing immunohistochemistry with an antibody to OLIG2 then quantifying cells that were positive for both EdU and OLIG2. Trained mice injected with C21 had significantly fewer cells with both EdU and OLIG2 staining compared to mice injected with vehicle control, implying that oligodendrogenesis was greatly impaired (Fig. 6C). Thus, we concluded that neuronal activity in the ACC is required for learning-induced oligodendrogenesis.

Discussion

This study showed that episodic learning, modeled by an IA paradigm in rats and mice, induces a rapid expression of the oligodendrocyte-specific mRNAs *olig2*, *myrf*, *mbp*, and *plp1* in the ACC but not in the dHC, though we did detect an increase in *enpp6* in the dHC. The reason for this increase in *enpp6* is unclear; ENPP6 is a choline phosphodiesterase involved in lipid metabolism and myelin biogenesis (Morita et al., 2016), and one possible explanation for its upregulation in the absence of changes in oligodendrogenesis markers is that ENPP6 in the hippocampus might be recruited by learning to regulate mechanisms of myelination and not oligodendrogenesis. In fact, whether existing myelin is remodeled after a learning experience is an open question.

Our western blot analyses confirmed that levels of OLIG2 significantly increased in the ACC following learning, supporting the idea that oligodendrogenesis is rapidly upregulated in this brain region in response to experience. Interestingly, MBP protein levels did not change, despite a significant increase in *mbp* mRNA levels. This dichotomy might be due to the fact that there is a large pool of MBP in the brain, so relatively small changes of MBP induced by a learning event may be difficult to be detected. Another oligodendrocyte-specific protein, CASPR, which is an axonal membrane protein involved in myelin sheet growth, significantly increased after learning in the ACC, confirming the idea that learning rapidly activates oligodendrocyte-specific mechanisms and myelination in that region. The upregulation of both mRNAs and proteins accompanied associative learning but were not found in unpaired behavioral

paradigms, which served as a control for the separate experiences of context and footshock, indicating that oligodendrocyte-mediated mechanisms are involved in associative memory processes.

Our results also extended previous findings on motor, spatial, and contextual fear memories by showing that global disruption of oligodendrogenesis impairs novel object location memories, strengthening the conclusion that oligodendrogenesis is a fundamental mechanism required for long-term memory formation.

Furthermore, by using multiple genetic and molecular approaches in rats and mice targeting specific brain regions of interest we provided evidence that Myrf-dependent oligodendrogenesis is required in the ACC but not the dHC, confirming the data across species. Thus, only certain brain regions in a given memory system recruit oligodendrogenesis for memory consolidation. To our knowledge, this is the first demonstration of a differential requirement for oligodendrogenesis in selected brain regions for memory formation, and specifically for hippocampus-dependent memories. Steadman et al. (2019) and Pan et al. (2020) recently reported that global *myrf* knockout prevents the formation of spatial and contextual memories. These studies showed that water maze and contextual fear conditioning learning in mice rapidly induce oligodendrocyte precursor cell (OPC) proliferation and differentiation into myelinating oligodendrocytes (OLs) in cortical regions such as the ACC and medial prefrontal cortex (mPFC), but not the hippocampus. They suggested that myelin remodeling following training might be restricted to brain regions associated with long-term consolidation of hippocampus-dependent memories. However, because these studies utilized a global knockout approach, they could not determine whether oligodendrogenesis in specific brain regions is required for memory formation. Identification of region- and circuitry-specific requirements for oligodendrogenesis and/or myelination in different types of learning and behavioral stimuli is important because it will offer critical knowledge for better understanding the role of myelin in healthy brain functions as well as in diseases. Such a knowledge will also expand our understanding of the circuitry that supports responses to learning.

Why oligodendrogenesis is required in the ACC but not the hippocampus is an open question, and one possible explanation is that oligodendrogenesis may subserve long-term changes required for memory

storage. It is known that in cortical regions including the ACC, but not in the hippocampus, episodic and spatial memories are stored for the very long term via a process that requires time and is known as system consolidation (Dudai et al., 2015). During system consolidation the memories that initially recruit hippocampus and cortical regions redistribute their representation: over time the hippocampus become dispensable, leaving cortical regions as the site of long-term memory storage (Frankland & Bontempi, 2005; Dudai et al., 2015; Squire et al., 2015) . Notably, other types of memory such as motor memories are stored long-term through a consolidation process in cortical areas and precisely in motor cortices (Attwell et al., 2002; Krakauer & Shadmehr, 2006). Further studies are needed to identify the region- and circuitry-specific oligodendrogenesis and myelination underlying the processes of consolidation of the various memory systems. For hippocampus-dependent memories, it is likely that other cortical regions in addition to the ACC recruit oligodendrogenesis. For example, similarly to the ACC, the mPFC is involved in hippocampus-dependent long-term memory consolidation (Frankland & Bontempi, 2005) and the induction of oligodendrogenesis has been found in the mPFC after spatial and contextual fear learning (Pan et al., 2020; Steadman et al., 2020). Whether there are differences in the regulation of oligodendrogenesis between the ACC and the mPFC remains to be investigated. Thus, in the context of this literature, our results lead us to speculate that myelination, which is a process that takes time and presumably leads to the stabilization of circuitry (Forbes & Gallo, 2017; Mount & Monje, 2017; Xin & Chan, 2020) may be a mechanism supporting the long-lasting memory storage, which in cortical regions persists for weeks, months, or even years. Whether the hippocampus is instructive for the cortical oligodendrogenesis changes induced by learning is possible and is in agreement with the findings that global oligodendrogenesis knockout impairs activity coupling between hippocampus and ACC. Indeed, Steadman (2019) and Pan (2020) both speculated that experience-dependent myelination might promote the coupling of ensembles across regions to support the generation of a coordinated memory network because when they blocked myelin formation throughout the brain, the activity and coordination in neural ensembles across the hippocampus and PFC networks was altered.

In the present study, we also dissected the requirement for oligodendrogenesis in various phases of memory. We found that oligodendrogenesis in the ACC is necessary for the consolidation process but not for the initial acquisition of memory (learning) or remote storage. In fact, inhibiting oligodendrogenesis before training did not affect short-term memory or acquisition, nor was there an effect on memory when oligodendrogenesis was inhibited at a remote time point. However, disruption of oligodendrogenesis after training impaired long-term memory tested one day later, and the impairment persisted when the memory was tested at remote time points, such as four weeks after training. The lack of an effect on memory when oligodendrogenesis is disrupted weeks after training agree with the results of Steadman et al. (2019), who showed that global knockout of *Myrf* at 25 days after water maze training did not impair memory retention. From these results, we can conclude that *MYRF*-dependent oligodendrogenesis in cortical regions is necessary for the rapid phase of consolidation, but not for learning, retrieval, or memory storage.

Our results also shed light on the kinetics of oligodendrogenesis requirement in recent memory recall. Steadman et al. (2019) found that *myrf* global knockout disrupts one-day-old spatial memory, and the disruption was still observed at a remote time point 28 days after training. By contrast, Pan et al. (2020) reported that *myrf* knockout mice trained in contextual fear conditioning (CFC) had intact recent memory recall at 1 day after training but impaired remote memories at 28 days after training. We found that global and ACC-targeted knockout of *myrf* in mice as well as ACC-specific ODN-mediated knockdown of MYRF in rats impaired recent memories, tested at one day after IA training. The impairments persisted in both rats and mice tested up to 28 days after training, leading us to conclude that MYRF-dependent oligodendrogenesis is rapidly upregulated and engaged following learning to selectively support a rapid phase of memory consolidation. It is possible that task-related differences in the kinetics of MYRF requirements exist, and that CFC has a slower cortical recruitment of oligodendrogenesis relative to water maze and IA tasks. Knowing the role of oligodendrogenesis in specific memory processes and temporal phases of memory provides valuable information for future development of temporally targeted treatments for cognitive symptoms of demyelinating diseases.

Finally, using a chemogenetic approach, we showed that the inhibition of neuronal activity in the ACC prevents learning-induced oligodendrogenesis. This demonstrated that oligodendrogenesis is triggered by neuronal activity and is in agreement with findings indicating that neuronal activity can drive adaptive myelination (Baraban et al., 2016; Mount & Monje, 2017; Noori et al., 2020). We speculate that neurons that are activated during learning engage oligodendrogenesis to produce *de novo* myelination that support formation and storage of the memory long term. Perhaps the activity-driven oligodendrogenesis reflect the activity-dependent changes in myelin patterning that have been hypothesized to promote coordinated reactivation of neural ensembles regulated by hippocampal-cortical synchronization and believed to underlie the consolidation of hippocampus-dependent memories (Pajevic et al., 2014).

In sum, our data support the view that activity-regulated oligodendrogenesis in selected brain regions underlies hippocampus-dependent memory consolidation. We suggest that this induced oligodendrogenesis provides the myelination necessary to support the stabilization process required to store information long-term.

Materials and Methods

Key resources table:

Reagent type (species) or resource	Designation	Source or reference	Identifiers	Concentration
Strain, strain background (R. norvegicus, male)	Crl:LE Long-Evans	Charles River	Cat# 2308852, RRID:RGD_2308852	
Strain, strain background (M. Musculus, male and female)	B6, B6J, B6/J	The Jackson Laboratory	Stock No: 000664	
Strain, strain background (M. Musculus, male and female)	B6.129S-Pdgfra$^{tm1.1(cre/ERT2)Blh}$/J	The Jackson Laboratory	Stock No: 032770	
Strain, strain background (M. Musculus, male and female)	B6;129-Myrf^{tm1Barr}/J	The Jackson Laboratory	Stock No: 010607	
Commercial assay or kit	Qiagen RNeasy Micro Kit	Qiagen	Cat# 74004	
Commercial assay or kit	Qiagen QuantiTect Rev. Transcription Kit	Qiagen	Cat# 205311	
Commercial assay or kit	Bio-Rad iQ SYBR Green Supermix	Bio-Rad	Cat# 1708880	
Commercial assay or kit	Bradford protein assay kit	Bio-Rad	Cat# 5000201	

antibody	Anti-Olig2	Millipore company	Cat# MABN50	WB: 1:1000; IHC: 1:1000
antibody	Anti-MBP	Millipore company	Cat# SKB3-05-675	WB: 1:500; IHC: 1:1000
antibody	Anti-Caspr	Millipore company	Cat# MABN69	WB: 1:2000
antibody	Anti-MAG	Cell Signaling	Cat# 9043S	WB: 1:1000
antibody	anti-Olig2	Millipore company	Cat# AB9610	IHC: 1:1000
antibody	anti-CC1	Calbiochem	Cat# OP80	IHC 1:500
antibody	anti-Pdgfrα	Cell signaling	Cat# 3461S	IHC: 1:1000
Commercial assay or kit	Click-iT™ Plus EdU Cell Proliferation Kit	Thermo Fisher Scientific	Cat# C20086	
Chemical compound, drug	5-ethynyl-2'-deoxyuridine	Biosynth	Cat# 087011802	80mg/kg
Chemical compound, drug	DAPI (4',6-Diamidino-2-Phenylindole, Dihydrochloride)	Life technologies	Cat# CD1306	1:10,000
antibody	Alexa Fluor® 647 Goat Anti-Mouse IgG (H+L)	Invitrogen	Cat# A21236	IF: 1:800
antibody	Alexa Fluor® 488 Goat anti-Rabbit IgG (H+L)	Invitrogen	Cat# A11034	IF: 1:800
antibody	Alexa Fluor ® 568	Invitrogen	Cat# A11036	IF: 1:800

	goat anti-rabbit IgG (H+L)			
Genetic reagent	pAAV-MBP-CreER^{T2}	Vector Biolabs	Cat# VB1545	AAV-PHP.B capsid; titer: 10x13 GC/μl
Genetic reagent	AAV-hSyn-hM4D(Gi)-mCherry	Addgene	Cat# 50475-AAV8	titer: 7×10^{12} vg/mL;
Chemical compound, drug	compound 21	Hello Bio	Cat#: HB6124	1mg/kg
Chemical compound, drug	Tamoxifen	Sigma-Aldrich	Cat# T5648	200mg/kg
Antibody	IRDye 680LT	LI-COR Biosciences	Cat# 926-68050, RRID:AB_2783642	WB (1:10000)
Antibody	IRDye 800CW (goat anti-rabbit)	LI-COR Biosciences	Cat# 926-32211, RRID:AB_621843	WB (1:10000)
Antibody	anti-β-actin	Santa Cruz Biotechnology	Cat# sc-47778 HRP, RRID:AB_2714189	WB (1:20000)
Software, algorithm	Adobe Illustrator C6	Adobe	https://www.adobe.com/products/illustrator.html	
Software, algorithm	R		http://cran.r-project.org/	
Software, algorithm	Image Studio Lite	LI-COR Biosciences	https://www.licor.com/bio/products/software/image_studio_lite/	

409

Rats

All animal procedures complied with the US National Institute of Health Guide for the Care and Use of Laboratory Animals and were approved by the New York University Animal Care Committees. Adult male Long–Evans (Charles Rivers, Wilmington, MA) rats weighing between 200 and 250 g were used. Animals were individually housed and maintained on a 12-h light/dark cycle. Experiments were performed during the light cycle. All rats were pair-housed and allowed ad libitum access to food and water and were handled for 3 minutes per day for 5 days before behavioral procedures. For all experiments, rats were randomly assigned to different groups. All protocols complied with the National Institutes of Health Guidelines for the Care and Use of Laboratory Animals and were approved by the Institutional Animal Care and Use Committee at New York University.

Mice

Male and female Pdgfrα-CreER^{T2}-Myrf floxed (P-Myrf) mice were obtained by crossing Pdgfra-CreER^{T2} (The Jackson Laboratory, Bar Harbor, ME; B6.129S-Pdgfra$^{tm1.1(cre/ERT2)Blh}$/J; Stock No: 032770), and Myrf floxed mice (The Jackson Laboratory, Bar Harbor, ME; B6;129-Myrf^{tm1Barr}/J; Stock No: 010607). Breeding was designed to produce P-Myrf$^{+/+}$, P-Myrf$^{flox/+}$ P-Myrf$^{flox/flox,}$ Myrf$^{+/+}$, Myrf$^{flox/+}$ Myrf$^{flox/flox}$ male and female littermates. Mice were bred in the animal facilities at New York University under a 12 h/12 h light/dark cycle (light on at 07.00 a.m.) with food and water ad libitum. After weaning, mice were group-housed (two to four per cage) in transparent plastic cages (31 × 17 × 14 cm) with free access to food and water. For inducing Cre-mediated knockout, all P-Myrf groups were administered 4 intraperitoneal (i.p.) injections of tamoxifen (TAM, Sigma-Aldrich St Louis, MO; Cat# T5648) dissolved in corn oil every other day at a dosage of 0.2g/kg of mouse. Mice were handled for 3 min per day for 5 days before behavioral procedures. For oligodendrogenesis experiments, c57/BL6 8–10-week males were used.

All mice were 8-10 weeks old at the start of behavioral assays. For all experiments, mice were randomly assigned to different groups. All protocols complied with the National Institutes of Health

436 Guide for the Care and Use of Laboratory Animals and were approved by the Institutional Animal Care
437 and Use Committee at New York University.
438
439 **Inhibitory Avoidance**
440 The paradigm employed a chamber (Med Associates Inc., St. Albans, VT), which consisted of a
441 rectangular Perspex box divided into a white light illuminated compartment and a dark black shock
442 compartment (each 20.3 cm × 15.9 cm × 21.3 cm) separated by a door. The chamber was located in a
443 sound-attenuated, red light illuminated room. During training and re-training sessions, the animal was
444 placed in the lit compartment with its head facing away from the door. After 10 seconds (s) for rats and
445 30s for mice, the door automatically opened, allowing the animal access to the dark compartment. The
446 door closed when the animal entered the dark compartment with all four limbs, and a foot shock (2 s,
447 0.9 mA in rats and 0.7mA in mice) was administered. The animal was removed from the dark
448 compartment (10 s after the shock for rats and immediately after for mice) and returned to its home cage.
449 Memory tests were performed at designated time points by placing the animal back in the lit compartment
450 and measuring their latency to enter the dark compartment. Foot shocks were not administered during
451 memory testing, and testing was terminated at 900s. Reminder foot shocks (R.S.), with identical duration
452 and intensity to those used in training (i.e., 2 s, 0.9 mA), were administered in a novel, neutral chamber
453 with transparent walls in a different experimental room. The animal was placed into the neutral chamber
454 for 10s before receiving a single R.S. The animal was removed from the chamber immediately after the
455 R.S. and returned to its home cage.
456 Control groups consisted of 1) untrained (U.T.) animals which were handled like the
457 experimental but, instead of undergoing training, remained in their home cage, and 2) unpaired (UP)
458 animals, which underwent the I.A. box exposure procedure without receiving a shock and, one hour later,
459 given a foot shock immediately after being placed on the grid of the dark chamber and then immediately
460 returned to the home cage.
461

Real-time quantitative PCR (RT-qPCR)

The bilateral dorsal hippocampus or ACC was dissected into TRIzol (Invitrogen, Waltham, MA). Total RNA was extracted from each animal sample using RNeasy Micro Kit (Qiagen, New Delhi, India, cat# 74004) and reverse-transcribed using Qiagen QuantiTect Rev. Transcription Kit (Cat# 205311). RT-PCR was done using a BioRad CFX96 Touch Real-Time PCR machine. Twenty ng of the first-strand cDNA was subjected to PCR amplification using Bio-Rad iQ SYBR Green Supermix (Bio-Rad Laboratories, Hercules, CA; Cat# 1708880). Forty cycles of PCR amplification were performed: denaturing at check cycle 95°C for 15 s, annealing at 60°C for 30 s, and extension for 20 s at 72°C. Triplicates were performed for each cDNA sample. Delta-delta CT method was used to determine the relative quantification of gene expression in trained and unpaired groups compared to untrained animals. Primer sequences used: Mbp (Forward, 5′ GGCAAGGACTCACACACAAGAA 3′; Reverse, 5′ CTTGGGTCCTCTGCGACTTC 3′), Plp1 (Forward, 5′ GCCAGAATGTATGGTGTTC 3′; Reverse, 5′ CAGCAATCATGAAGGTGAG 3′), Myrf (Forward, 5′ CCACATCAGCAGAACAAGTG 3′; Reverse, 5′ ACACGATAGGTGAGCATAGG 3′), Mag (Forward, 5′ CTGTGGTCGCCTTTG 3′; Reverse, 5′ GCTCTCAGTGACAATCC 3′), Olig2 (Forward, 5′ CACGTCTTCCACCAAGAAAG 3′; Reverse, 5′ GTCCATGGCGATGTTGAG 3′), Enpp6 (Forward, 5′ TGTGAGGTCCACCAGATG 3′; Reverse, 5′ CCCGATGTCGAATGACTTG 3′), Erbb3 (Forward, 5′ CTGGCGTCTTTGGAACTG 3′; Reverse, 5′ GCAGACTGGAATCTTGATGG 3′), Arc (Forward, 5′ CCCTGCAGCCCAAGTTCAAG 3′; Reverse, 5′ GAAGGCTCAGCTGCCTGCTC 3′). Erg1 (Forward, 5′ ACCTACCAGTCCCAACTCATC 3′; Reverse, 5′ GACTCAACAGGGCAAGCATAC 3′). Cfos (Forward, 5′ ATCCTTGGAGCCAGTCAAGA 3′; Reverse, 5′ ATGATGCCGGAAACAAGAAG 3′) and Gapdh (Forward, 5′GAACATCATCCCTGCATCCA 3′; Reverse 5′CCAGTGAGCTTCCCGTTCA 3′) was used as an internal control.

Western Blot Analysis

Rats were euthanized, and their brains were quickly removed and snap-frozen with pre-chilled 2-methyl butane on dry ice. Dorsal hippocampal and ACC punches were obtained with a neuro punch (19 gauge; Fine Science Tools, Foster City, CA) from frozen brains mounted on a cryostat at -20°C and isolated the bilateral regions per animal (individual animal sample). Individual animal samples were homogenized in ice-cold RIPA buffer (50 mM Tris base, 150 mM NaCl, 0.1% SDS, 0.5% Na-deoxycholate, 1% NP-40) with protease and phosphatase inhibitors (0.5 mM PMSF, 2 mM DTT, 1 mM EGTA, 2 mM NaF, 1 µM microcystin, 1 mM benzamidine, 1 mM sodium orthovanadate, and Sigma-Aldrich protease and phosphatase inhibitor cocktails). Protein concentrations were determined using the Bio-Rad protein assay (Bio-Rad Laboratories, Hercules, CA, USA). Equal amounts of total protein extract per sample (20 µg) were resolved on denaturing SDS-PAGE gels and transferred to the Immobilon-FL Transfer membrane (Bio-Rad Laboratories, Hercules, CA, USA) by electroblotting. Membranes were dried, reactivated in methanol, washed with water, and then blocked in the Biorad blocking buffer for 2 h at room temperature. The membranes were then incubated with primary antibody overnight at 4°C in the buffer recommended by the antibody manufacturer. The membranes were then washed with TBS containing 0.2% Tween-20 (TBST) and incubated with species-appropriate fluorescently conjugated secondary antibody goat anti-mouse IRDye 680LT (1:10,000) or goat anti-rabbit IR Dye 800CW (1:10,000) from LI-COR Bioscience (Lincoln, NE, USA)] for 2 h at room temperature. Membranes were again washed in TBST and finally scanned to detect immunoreactivities using the Odyssey Infrared Imaging System (Li-Cor Bioscience). Data were quantified using pixel intensities with the Odyssey software (Li-Cor) according to the manufacturer's protocols. The following antibodies were used at the indicated dilutions: Anti-Olig2 (1:1000, MilliporeSigma, Burlington, MAcat# MABN50), Anti-MBP (1:500, MilliporeSigma, Burlington, MA; cat# SKB3-05-675), Anti-Caspr (1:2,000, MilliporeSigma, Burlington, MA; cat# MABN69), and Anti-MAG (1:1,000, Cell signaling, Danvers MA; cat# 9043S). Anti-β-Actin (1:20,000, Santa Cruz Biotechnology, Dallas, TX, USA; cat# sc-47778) was used as a loading control for all blots.

513 **Immunofluorescent staining**

514 Mice were anesthetized with an intraperitoneal (i.p.) injection of 750 mg/kg chloral hydrate and
515 transcardially perfused with 4% paraformaldehyde in PBS pH 7.4. Their brains were post-fixed in PBS
516 pH 7.4 overnight at 4°C, followed by PBS pH 7.4 with 30% sucrose for 72 h. 20 µm coronal brain
517 sections were collected by cryosection for free-floating immunofluorescent staining. The sections were
518 then incubated with the blocking solution (PBS pH 7.4 with 0.4% Triton X-100, 5% normal goat serum,
519 1% bovine serum albumin) for 2 h at room temperature, followed by incubation with the primary
520 antibody. Primary antibodies: rabbit anti-Olig2 antibody (1:1000, EMD MilliporeSigma, Burlington, MA;
521 Cat# AB9610), mouse anti-Olig2 antibody (1:1000, EMD MilliporeSigma, Cat# MABN50), mouse anti-
522 CC1 antibody (1:500, Calbiochem, cat# OP80), mouse anti MBP Antibody (1:1000, EMD
523 MilliporeSigma , Cat# 06-675) or anti-Pdgfrα antibody (1:1000, Cell signaling, Danvers MA, cat#
524 3461S). Sections were incubated with primary antibodies diluted in the blocking solution for 48 h at 4°C.
525 Subsequently, the brain sections were washed in PBS 0.4% Triton three times and then incubated with
526 goat anti-rabbit or goat anti-mouse Alexa Fluor-568, Alexa Fluor-488, or Alexa Fluor-647 secondary
527 antibodies (1:800, Invitrogen, Waltham, MA) for 2 h at room temperature. 5-ethynyl-2'-deoxyuridine
528 (EdU) was incubated using Click-iT™ Plus EdU Cell Proliferation Kit (Thermo Fisher Scientific) after
529 DAPI staining. Sections were mounted with Prolong Diamond antifade mountant (Invitrogen, Waltham,
530 MA). Three sections, representing rostral, medial, and caudal ACC (+.98mm, +.5mm, and -.10mm
531 bregma), and hippocampus (-1.3mm, -1.8mm, and -2.5mm bregma) were analyzed for each set of
532 staining. One image per hemisphere per bregma section for each animal was captured by a Leica TCS
533 SP5 confocal microscope (Leica, Wetzlar, Germany) at 20x. Quantification was performed using the
534 ImageJ software (U.S. National Institutes of Health) blinded to the experimental conditions using
535 automated custom macro programs. For 5-ethynyl-2'-deoxyuridine (EdU) quantification, mice were
536 injected intraperitoneally with EdU (80mg/kg) dissolved in 7.4 PH phosphate-buffered saline. To stain for
537 EdU we used Click-iT™ Plus EdU Cell Proliferation Kit (Thermo Fisher Scientific) after DAPI staining
538 on brain sections.

539

540 **Rat cannula implants and injections**

541 Rats were anesthetized with ketamine (75 mg/kg) mixed with xylazine (10 mg/kg), and stainless-
542 steel guide cannulas (C313G-SPC; 26-gauge P1 Technologies, Roanoke, VA) were implanted bilaterally
543 using a stereotaxic apparatus (Kopf Instruments, Tujunga, CA) through holes drilled in the overlying
544 skull to target the ACC (0.2 mm anterior, 0.5 mm lateral, -1.3 mm ventral from bregma). The
545 guide cannulas were fixed to the skull with dental cement. Rats were administered meloxicam (3 mg/kg,
546 subcutaneous) and let recover for at least 14 days before undergoing behavioral experiments. The
547 injections were conducted using a 33-gauge needle, extending 1.5 mm beyond the tip of the
548 guide cannulas, and connected via a polyethylene tubing (PE50) to a 1 µl Hamilton (Reno, NV) syringe
549 controlled by an infusion pump (Harvard Apparatus. Holliston, MA) 2 nmol of antisense
550 oligodeoxynucleotides (AS-ODN) or the relative scrambled sequence (SCR-ODN) were delivered per
551 brain hemisphere in 0.5 µl of PBS (pH 7.4) at a rate of 0.333 µl/min. Sequences were as follows: Myrf AS
552 5′-GGTCTCGTCCACCACCTCCAT-3′; Myrf SCR 5′-CCATCTTCCGACGTTCGACCC-3′. The SCR-
553 ODN, which served as control, contained the same relative AS-ODN base composition but in random
554 order and showed no homology to any mammalian sequence in the GenBank database, as confirmed
555 using a basic local alignment search tool (BLAST). All ODNs were phosphorothioated on the three-
556 terminal bases at each end to protect against nuclease degradation. ODNs were synthesized, reverse-phase
557 cartridges purified, and purchased from Gene Link (Hawthorne, NY). Rats were euthanized at the end of
558 the behavioral experiments to confirm cannula and injection placement. Toward this end, 40 µm coronal
559 sections were sliced following fixation of the brains in 10% formalin; then, the sections were examined
560 under a light microscope to verify cannula placement. Rats with incorrect placement were excluded from
561 the study.

562

563 **Object location memory**

564 Mice were habituated, trained, and tested in a square, open field (29 × 29 × 18 cm) with white
565 Plexiglas walls and floor measured at 12.5 (±2.5) lux in the center of a dim room. Visual cues were
566 provided within the box and on the walls of the room. Behavior was recorded with a video camera
567 positioned above the arena. Mice were first habituated to the arena for 10 minutes for 3 consecutive days
568 before the training. Twenty-four hours after the last habituation session, each animal was returned to the
569 arena for its training session. Training consisted of exposing the mice to two identical objects constructed
570 from Mega Bloks (Montreal, Canada) secured to the floor of the arena. Object sizes were no taller than
571 twice the size of the mice. Mice were initially placed facing a corner, away from the objects, and were
572 allowed to explore the arena and objects for 10 min. 4 hours after training; each animal was tested in the
573 arena. During testing, one object remained in the same location as during training, whereas the second
574 object had been moved to a novel location. Animals were placed in the arena facing the same direction as
575 during training and were allowed to explore for 10 min. The placement of the object in the novel location
576 was counterbalanced between subjects. The arena and objects were cleaned between sessions. Video files
577 were coded and scrambled. The experimenter was blind to treatment and scored the total time the mice
578 spent actively exploring each object in each session. Active exploration was defined as the mice pawing
579 at, sniffing, or whisking with their snout directed at the object from a distance of less than ∼1 cm. Sitting
580 on or next to an object was not counted as active exploration. Mice with less than 10s total exploration
581 time were excluded. If mice explored more than 15s, the exploration percentage was taken at 15s of total
582 exploration time. Memory was measured as the percentage of time spent exploring the object in the novel
583 location compared with the stationary object.
584
585 **Open field**
586 Mice were allowed to freely explore an open-field arena illuminated at 195 lux. (43.2 cm × 43.2
587 cm × 30.5 cm (Med Associates Inc., St. Albans, VTENV-515) for 10 min. The open field was designated
588 into 2 sections: center box and outer border. Percentage time spent in the center and average velocity and

589 total distance were quantified. Activity was analyzed with Ethovision-XT (Noldus Information
590 Technology).
591
592 **Mouse viral injections and C21 administration**
593 Mice were anesthetized with isoflurane. The skull was exposed, and holes were drilled in the
594 skull bilaterally above the ACC or dHC. A Hamilton (Reno, NV) syringe with a 33 gauge needle,
595 mounted onto a nanopump (K.D. Scientific, Holliston, MA), 0.2ul microliters of the virus was injected
596 per mouse bilaterally into the ACC (+ 0.5mm anterior to bregma, ± 0.3 lateral of bregma, -2 dorsal of
597 skull surface) or 1ul per mouse bilaterally into the dorsal hippocampus (+1.7mm anterior to bregma ±1.5
598 lateral of bregma -1.75 dorsal of skull surface) at a rate of 0.2µL/min. The injection needle was left in
599 place for 5 min following injection to allow complete dispersion of the solution and then the scalp was
600 sutured. Meloxicam (3 mg/kg) was used as an analgesic treatment after surgeries, and mice were allowed
601 to recover for 14 days before training.
602 The pAAV-MBP-CreER^{T2} virus (titer: 10x13 GC/µl) was packaged into AAV-PHP.B capsid and
603 purchased from Vector Biolabs (Malvern, PA, cat# VB1545). The AAV-hSyn-hM4D(Gi)-mCherry (cat#
604 VB1545) was purchased from add gene (titer: 7×10^{12} vg/mL; cat# 50475-AAV8). C21 (HB6124, Hello
605 Bio, Princeton, NJ) was dissolved in PBS pH7.4 and injected at 1mg/kg 60 min before training. After
606 behavioral experiments, mice were anesthetized with an i.p. injection of 750 mg/kg chloral hydrate and
607 transcardially perfused with 4% paraformaldehyde in PBS pH 7.4. Their brains were post-fixed in this
608 solution overnight at 4°C, followed by PBS pH7.4 with 30% sucrose for 72 h. 30 µm brain sections were
609 collected by cryosection for free-floating immunofluorescent staining.
610
611 **Statistical analyses**
612 Data were statistically analyzed using Prism software. The student's t-test was used to compare
613 statistical differences between two experimental groups. When more than two groups were compared,
614 data were analyzed with one- or two-way repeated-measure ANOVA followed by Bonferroni post hoc

test. All values represent the mean ± standard error of the mean (SEM). The experimental n, the statistical test used, and the statistical significance are indicated in figure legends. The Excel-based PCR Array Data Analysis was used to analyze the qPCR results. The number of independent experiments carried out and the numbers of biological replicates [i.e., animals (n)] are indicated in each figure legend. No statistical method was used to predetermine sample size. The numbers of subjects used in our experiments were the minimum required to obtain statistical significance, based on our experience with the behavioral paradigm and in agreement with standard literature.

Acknowledgments

We thank Dr. James Salzer (New York University School of Medicine) for providing an initial group on transgenic mice and for helpful discussions. This work was supported by NIH grants R37MH065635 to CMA, HHMI Gilliam fellowship to LPB. ON was supported by NIGMS MARC grant 5T34GM008078.

Author contributions

LPB, CMA, designed the study. LPB, BB, and ON performed the experiments. LPB and CMA wrote the manuscript.

Ethics

All animal procedures complied with the US National Institute of Health Guide for the Care and Use of Laboratory Animals and were approved by the New York University Animal Care Committees. All surgeries were performed under isoflurane anesthesia and every effort was made to minimize suffering.

Competing interests

The authors declare that no competing interests exist.

641 **References**

642 Adamsky, A., & Goshen, I. (2018, Feb 1). Astrocytes in Memory Function: Pioneering Findings and
643 Future Directions. *Neuroscience, 370*, 14-26. DOI:10.1016/j.neuroscience.2017.05.033

644

645 Attwell, P. J. E., Cooke, S. F., & Yeo, C. H. (2002). Cerebellar Function in Consolidation of a Motor
646 Memory. *Neuron, 34*(6), 1011-1020. DOI:10.1016/s0896-6273(02)00719-5

647

648 Bambah-Mukku, D., Travaglia, A., Chen, D. Y., Pollonini, G., & Alberini, C. M. (2014, Sep 10). A
649 positive autoregulatory BDNF feedback loop via C/EBPbeta mediates hippocampal memory
650 consolidation. *J Neurosci, 34*(37), 12547-12559. DOI:10.1523/JNEUROSCI.0324-14.2014

651

652 Baraban, M., Mensch, S., & Lyons, D. A. (2016, Jun 15). Adaptive myelination from fish to man. *Brain*
653 *Res, 1641*(Pt A), 149-161. DOI:10.1016/j.brainres.2015.10.026

654

655 Bramham, C. R., Alme, M. N., Bittins, M., Kuipers, S. D., Nair, R. R., Pai, B., Panja, D., Schubert, M.,
656 Soule, J., Tiron, A., & Wibrand, K. (2010, Jan). The Arc of synaptic memory. *Exp Brain Res,*
657 *200*(2), 125-140. DOI:10.1007/s00221-009-1959-2

658

659 Bujalka, H., Koenning, M., Jackson, S., Perreau, V. M., Pope, B., Hay, C. M., Mitew, S., Hill, A. F., Lu,
660 Q. R., Wegner, M., Srinivasan, R., Svaren, J., Willingham, M., Barres, B. A., & Emery, B.
661 (2013). MYRF is a membrane-associated transcription factor that autoproteolytically cleaves to
662 directly activate myelin genes. *PLoS Biol, 11*(8), e1001625. DOI:10.1371/journal.pbio.1001625

663

664 Chen, D. Y., Stern, S. A., Garcia-Osta, A., Saunier-Rebori, B., Pollonini, G., Bambah-Mukku, D., Blitzer,
665 R. D., & Alberini, C. M. (2011, Jan 27). A critical role for IGF-II in memory consolidation and
666 enhancement. *Nature, 469*(7331), 491-497. DOI:10.1038/nature09667

667

668 Chen, M. B., Jiang, X., Quake, S. R., & Sudhof, T. C. (2020, Nov). Persistent transcriptional programmes
669 are associated with remote memory. *Nature, 587*(7834), 437-442. DOI:10.1038/s41586-020-
670 2905-5

671

672 Dudai, Y., Karni, A., & Born, J. (2015, Oct 7). The Consolidation and Transformation of Memory.
673 *Neuron, 88*(1), 20-32. DOI:10.1016/j.neuron.2015.09.004

674

675 Einheber, S., Zanazzi, G., Ching, W., Scherer, S., Milner, T. A., Peles, E., & Salzer, J. L. (1997, Dec 15).
676 The axonal membrane protein Caspr, a homologue of neurexin IV, is a component of the septate-
677 like paranodal junctions that assemble during myelination. *J Cell Biol, 139*(6), 1495-1506.
678 DOI:10.1083/jcb.139.6.1495

679

680 Emery, B. (2013, Oct). Playing the field: Sox10 recruits different partners to drive central and peripheral
681 myelination. *PLoS Genet, 9*(10), e1003918. DOI:10.1371/journal.pgen.1003918

682

683 Forbes, T. A., & Gallo, V. (2017, Sep). All Wrapped Up: Environmental Effects on Myelination. *Trends*
684 *Neurosci, 40*(9), 572-587. DOI:10.1016/j.tins.2017.06.009

685
686 Frankland, P. W., & Bontempi, B. (2005, Feb). The organization of recent and remote memories. *Nat Rev*
687 *Neurosci, 6*(2), 119-130. DOI:10.1038/nrn1607

688
689 Garcia-Osta, A., Tsokas, P., Pollonini, G., Landau, E. M., Blitzer, R., & Alberini, C. M. (2006, Jul 26).
690 MuSK expressed in the brain mediates cholinergic responses, synaptic plasticity, and memory
691 formation. *J Neurosci, 26*(30), 7919-7932. DOI:10.1523/JNEUROSCI.1674-06.2006

692
693 Gerlai, R., Wojtowicz, J. M., Marks, A., & Roder, J. (1995, Jan-Feb). Overexpression of a calcium-
694 binding protein, S100 beta, in astrocytes alters synaptic plasticity and impairs spatial learning in
695 transgenic mice. *Learn Mem, 2*(1), 26-39. DOI:10.1101/lm.2.1.26

696
697 Gibson, E. M., Purger, D., Mount, C. W., Goldstein, A. K., Lin, G. L., Wood, L. S., Inema, I., Miller, S.
698 E., Bieri, G., Zuchero, J. B., Barres, B. A., Woo, P. J., Vogel, H., & Monje, M. (2014, May 2).
699 Neuronal activity promotes oligodendrogenesis and adaptive myelination in the mammalian
700 brain. *Science, 344*(6183), 1252304. DOI:10.1126/science.1252304

701
702 Gold, P. E. (1986). The use of avoidance training in studies of modulation of memory storage. *Behavioral*
703 *and Neural Biology, 46*(1), 87-98. DOI:10.1016/s0163-1047(86)90927-1

704
705 Heyward, F. D., & Sweatt, J. D. (2015, Oct). DNA Methylation in Memory Formation: Emerging
706 Insights. *Neuroscientist, 21*(5), 475-489. DOI:10.1177/1073858415579635

707
708 Hughes, E. G., Orthmann-Murphy, J. L., Langseth, A. J., & Bergles, D. E. (2018, May). Myelin
709 remodeling through experience-dependent oligodendrogenesis in the adult somatosensory cortex.
710 *Nat Neurosci, 21*(5), 696-706. DOI:10.1038/s41593-018-0121-5

711
712 Jendryka, M., Palchaudhuri, M., Ursu, D., van der Veen, B., Liss, B., Katzel, D., Nissen, W., & Pekcec,
713 A. (2019, Mar 14). Pharmacokinetic and pharmacodynamic actions of clozapine-N-oxide,
714 clozapine, and compound 21 in DREADD-based chemogenetics in mice. *Sci Rep, 9*(1), 4522.
715 DOI:10.1038/s41598-019-41088-2

716
717 Kandel, E. R., Dudai, Y., & Mayford, M. R. (2014, Mar 27). The molecular and systems biology of
718 memory. *Cell, 157*(1), 163-186. DOI:10.1016/j.cell.2014.03.001

719
720 Katzman, A., Khodadadi-Jamayran, A., Kapeller-Libermann, D., Ye, X., Tsirigos, A., Heguy, A., &
721 Alberini, C. M. (2021, Mar 24). Distinct Transcriptomic Profiles in the Dorsal Hippocampus and
722 Prelimbic Cortex Are Transiently Regulated following Episodic Learning. *J Neurosci, 41*(12),
723 2601-2614. DOI:10.1523/JNEUROSCI.1557-20.2021

724
725 Krakauer, J. W., & Shadmehr, R. (2006, Jan). Consolidation of motor memory. *Trends Neurosci, 29*(1),
726 58-64. DOI:10.1016/j.tins.2005.10.003

Luo, M., Yin, Y., Li, D., Tang, W., Liu, Y., Pan, L., Yu, L., & Tan, B. (2021, Jan). Neuronal activity-dependent myelin repair promotes motor function recovery after contusion spinal cord injury. *Brain Res Bull, 166*, 73-81. DOI:10.1016/j.brainresbull.2020.11.009

McKenzie, I. A., Ohayon, D., Li, H., de Faria, J. P., Emery, B., Tohyama, K., & Richardson, W. D. (2014, Oct 17). Motor skill learning requires active central myelination. *Science, 346*(6207), 318-322. DOI:10.1126/science.1254960

Morita, J., Kano, K., Kato, K., Takita, H., Sakagami, H., Yamamoto, Y., Mihara, E., Ueda, H., Sato, T., Tokuyama, H., Arai, H., Asou, H., Takagi, J., Ishitani, R., Nishimasu, H., Nureki, O., & Aoki, J. (2016, Feb 18). Structure and biological function of ENPP6, a choline-specific glycerophosphodiester-phosphodiesterase. *Sci Rep, 6*, 20995. DOI:10.1038/srep20995

Morris, G. P., Clark, I. A., Zinn, R., & Vissel, B. (2013, Oct). Microglia: a new frontier for synaptic plasticity, learning and memory, and neurodegenerative disease research. *Neurobiol Learn Mem, 105*, 40-53. DOI:10.1016/j.nlm.2013.07.002

Mount, C. W., & Monje, M. (2017, Aug 16). Wrapped to Adapt: Experience-Dependent Myelination. *Neuron, 95*(4), 743-756. DOI:10.1016/j.neuron.2017.07.009

Mumby, D. G., Gaskin, S., Glenn, M. J., Schramek, T. E., & Lehmann, H. (2002, Mar-Apr). Hippocampal damage and exploratory preferences in rats: memory for objects, places, and contexts. *Learn Mem, 9*(2), 49-57. DOI:10.1101/lm.41302

Noori, R., Park, D., Griffiths, J. D., Bells, S., Frankland, P. W., Mabbott, D., & Lefebvre, J. (2020, Jun 16). Activity-dependent myelination: A glial mechanism of oscillatory self-organization in large-scale brain networks. *Proc Natl Acad Sci U S A, 117*(24), 13227-13237. DOI:10.1073/pnas.1916646117

Okuno, H., Akashi, K., Ishii, Y., Yagishita-Kyo, N., Suzuki, K., Nonaka, M., Kawashima, T., Fujii, H., Takemoto-Kimura, S., Abe, M., Natsume, R., Chowdhury, S., Sakimura, K., Worley, P. F., & Bito, H. (2012, May 11). Inverse synaptic tagging of inactive synapses via dynamic interaction of Arc/Arg3.1 with CaMKIIbeta. *Cell, 149*(4), 886-898. DOI:10.1016/j.cell.2012.02.062

Pajevic, S., Basser, P. J., & Fields, R. D. (2014, Sep 12). Role of myelin plasticity in oscillations and synchrony of neuronal activity. *Neuroscience, 276*, 135-147. DOI:10.1016/j.neuroscience.2013.11.007

Pan, S., Mayoral, S. R., Choi, H. S., Chan, J. R., & Kheirbek, M. A. (2020, Apr). Preservation of a remote fear memory requires new myelin formation. *Nat Neurosci, 23*(4), 487-499. DOI:10.1038/s41593-019-0582-1

Pezze, M. A., Marshall, H. J., Domonkos, A., & Cassaday, H. J. (2016, Feb 4). Effects of dopamine D1 modulation of the anterior cingulate cortex in a fear conditioning procedure. *Prog Neuropsychopharmacol Biol Psychiatry, 65*, 60-67. DOI:10.1016/j.pnpbp.2015.08.015

Rivers, L. E., Young, K. M., Rizzi, M., Jamen, F., Psachoulia, K., Wade, A., Kessaris, N., & Richardson, W. D. (2008, Dec). PDGFRA/NG2 glia generate myelinating oligodendrocytes and piriform projection neurons in adult mice. *Nat Neurosci, 11*(12), 1392-1401. DOI:10.1038/nn.2220

Saunders, A., Macosko, E. Z., Wysoker, A., Goldman, M., Krienen, F. M., de Rivera, H., Bien, E., Baum, M., Bortolin, L., Wang, S., Goeva, A., Nemesh, J., Kamitaki, N., Brumbaugh, S., Kulp, D., & McCarroll, S. A. (2018, Aug 9). Molecular Diversity and Specializations among the Cells of the Adult Mouse Brain. *Cell, 174*(4), 1015-1030 e1016. DOI:10.1016/j.cell.2018.07.028

Shepherd, J. D., & Bear, M. F. (2011, Mar). New views of Arc, a master regulator of synaptic plasticity. *Nat Neurosci, 14*(3), 279-284. DOI:10.1038/nn.2708

Sherman, D. L., & Brophy, P. J. (2005, Sep). Mechanisms of axon ensheathment and myelin growth. *Nat Rev Neurosci, 6*(9), 683-690. DOI:10.1038/nrn1743

Simons, M., & Nave, K. A. (2015, Jun 22). Oligodendrocytes: Myelination and Axonal Support. *Cold Spring Harb Perspect Biol, 8*(1), a020479. DOI:10.1101/cshperspect.a020479

Squire, L. R., Genzel, L., Wixted, J. T., & Morris, R. G. (2015, Aug 3). Memory consolidation. *Cold Spring Harb Perspect Biol, 7*(8), a021766. DOI:10.1101/cshperspect.a021766

Steadman, P. E., Xia, F., Ahmed, M., Mocle, A. J., Penning, A. R. A., Geraghty, A. C., Steenland, H. W., Monje, M., Josselyn, S. A., & Frankland, P. W. (2020, Jan 8). Disruption of Oligodendrogenesis Impairs Memory Consolidation in Adult Mice. *Neuron, 105*(1), 150-164 e156. DOI:10.1016/j.neuron.2019.10.013

Suzuki, A., Stern, S. A., Bozdagi, O., Huntley, G. W., Walker, R. H., Magistretti, P. J., & Alberini, C. M. (2011, Mar 4). Astrocyte-neuron lactate transport is required for long-term memory formation. *Cell, 144*(5), 810-823. DOI:10.1016/j.cell.2011.02.018

Taubenfeld, S. M., Wiig, K. A., Monti, B., Dolan, B., Pollonini, G., & Alberini, C. M. (2001). Fornix-Dependent Induction of Hippocampal CCAAT Enhancer-Binding Protein β and δ Co-Localizes with Phosphorylated cAMP Response Element-Binding Protein and Accompanies Long-Term Memory Consolidation. *The Journal of Neuroscience, 21*(1), 84-91. DOI:10.1523/jneurosci.21-01-00084.2001

Tran, F. H., Spears, S. L., Ahn, K. J., Eisch, A. J., & Yun, S. (2020, Nov 20). Does chronic systemic injection of the DREADD agonists clozapine-N-oxide or Compound 21 change behavior relevant to locomotion, exploration, anxiety, and depression in male non-DREADD-expressing mice? *Neurosci Lett, 739*, 135432. DOI:10.1016/j.neulet.2020.135432

Wang, F., Ren, S. Y., Chen, J. F., Liu, K., Li, R. X., Li, Z. F., Hu, B., Niu, J. Q., Xiao, L., Chan, J. R., & Mei, F. (2020, Apr). Myelin degeneration and diminished myelin renewal contribute to age-related deficits in memory. *Nat Neurosci, 23*(4), 481-486. DOI:10.1038/s41593-020-0588-8

Weible, A. P., Rowland, D. C., Pang, R., & Kentros, C. (2009, Oct). Neural correlates of novel object and novel location recognition behavior in the mouse anterior cingulate cortex. *J Neurophysiol, 102*(4), 2055-2068. DOI:10.1152/jn.00214.2009

Xin, W., & Chan, J. R. (2020, Dec). Myelin plasticity: sculpting circuits in learning and memory. *Nat Rev Neurosci, 21*(12), 682-694. DOI:10.1038/s41583-020-00379-8

Yirmiya, R., & Goshen, I. (2011, Feb). Immune modulation of learning, memory, neural plasticity and neurogenesis. *Brain Behav Immun, 25*(2), 181-213. DOI:10.1016/j.bbi.2010.10.015

Figure Legends

Figure. 1 Learning rapidly induces oligodendrocyte-specific mRNAs and proteins. (A) Schematic representation showing the experimental design: rats underwent IA training and were euthanized at 1 hour (1H), 1 day (1D), or 7 days (7D) after training and assessed with RT-qPCR. (B) RT-qPCR of *arc* performed in ACC extracts from untrained (UT) and trained rats euthanized at the timepoints indicated in A. (C) ACC and (D) dHC RT-qPCR analyses of the oligodendrocyte differentiation and myelin biogenesis genes *olig2*, *myrf*, *enpp6*, *mbp*, *mag* and *plp1*. Data are expressed as mean percentage ± s.e.m. of the untrained group (UT). Unpaired (UP) controls were added in groups where significant upregulation of oligodendrocyte genes were found. N = 4-12 per group; one-way ANOVA followed by Dunnett's multiple comparison test; 2 independent experiments. (E-H) Examples and densitometric western blot analyses of MBP, MAG, CASPR, and OLIG2 obtained from ACC total extracts from trained rats euthanized at time points mentioned in A, compared to respective age-matched UT controls. UP controls were included at the one-day post training timepoint. Data presented as mean percentage ± s.e.m. of untrained rats (n = 4-12 rats per group; two-tailed t-test; full Blot images can be found in Source Data file 2). (I) Examples of immunofluorescent staining of OLIG2 in the ACC of rats euthanized 1D after IA compared to UT control. Cumulative distribution of OLIG2 intensity measured from nuclei of ACC from

UT and trained rats perfused 1 day (1D) after training (n = 1678 and 1410 cell across four rats in UT and 1D groups respectively; two-tailed t-test; P<0.001). Mean values ± s.e.m. of the total number of OLIG2+ cells—data presented as positive cells per mm^2. Each dot represents the quantification of one image taken from the ACC. 4-6 images were taken per rat per side on a total of 4 rats [UT (n = 23) and Trained1D (n=20)]; two-tailed t-test; * indicates p<0.05, ** indicates p<0.01*** indicates p<0.001. For detailed statistical information, see Table 1-Source Data1.

Figure 2. Learning increases oligodendrogenesis in the ACC but not the dHC. Mice were injected with 5-ethynyl-2'-deoxyuridine (EdU), trained in IA, and perfused one day after training. (A) Representative immunohistochemical staining and relative quantifications for (upper panel) doubly stained EdU and Pdgfrα cells and (lower panel) and triple staining of EdU, Olig2 and CC1 to quantify OPC proliferation and differentiation, respectively. For each mouse, (A) ACC, (B) dHC, including CA1, CA2, CA3, and DG regions. Three coronal sections were quantified and averaged. In each coronal section the entire ACC and dHC were quantified bilaterally. Each dot in the graphs represents the average values of the three coronal section of each mouse. Data are presented as mean percentage ± s.e.m. of positive cell number relative to Dapi+ nuclei (scale bars: 40 μm; n = 4 mice per group, two-tailed t-test; *indicates P < 0.05). For detailed statistical information, see supplementary Table 2-Source Data1.

Figure 3. Global knockout of myrf results in long-term memory impairment. P-$Myrf^{+\backslash+}$ (*n* = 3) and P-$Myrf^{flox\backslash flox}$ (*n* = 5) littermates received one injection of tamoxifen (TAM) every other day for four times. Seven days after the last injection the mice underwent IA training. EdU was administered immediately before training and the mice were perfused one day after training. (A) Representative images and quantifications of ACC triple immunostaining (scale bar:40 μm) of EdU, Olig2 and CC1. For each mouse, three coronal sections were quantified and averaged. In each coronal section the entire ACC was quantified bilaterally. Each dot represents the average of the three coronal section of each mouse. Data are presented as mean percentage ± s.e.m. of positive cell number relative to Dapi+ nuclei (scale bars: 40

μm;, two-tailed t-test;). (B, C) P-Myrf$^{+\backslash+}$ and P-Myrf$^{flox\backslash flox}$ littermates were injected with TAM every other day for four injections terminating seven days before training. Mice were trained in IA and either tested at (B) 1, 7- and 28-days post-training (*n* = 10,11 per P-Myrf$^{+\backslash+}$ and P-Myrf$^{flox\backslash flox}$ per respectively) or (C) only at 28 days post-training *(n* = 13,6 per P-Myrf$^{+\backslash+}$ and P-Myrf$^{flox\backslash flox}$ groups respectively). (D) P-Myrf$^{+\backslash+}$ (*n* = 9) and P-Myrf$^{flox\backslash flox}$ (*n* = 8) littermates were trained and received tamoxifen injections starting 14 days after training and terminating seven days before testing, which occurred at 28D, 36D, and 56D post-training. Data are represented as mean latency ± s.e.m. (In seconds, s) (two-way ANOVA followed by Bonferroni *post hoc* test). (E) P-Myrf$^{+\backslash+}$ (*n* = 12) and P-Myrf$^{flox\backslash flox}$ (*n* = 8) littermates were injected four times with tamoxifen once every other day. Seven days after the last injection the mice underwent novel object location training and were tested 4 hours later (two-way ANOVA followed by Bonferroni *post hoc* test). (F) Open field test expressed as mean ±s.e.m. of (i) percent time spent in the center of the arena, (ii) total distance, and (iii) mean velocity exploring the arena. (n = 9,12 mice per P-Myrf$^{+\backslash+}$ and P-Myrf$^{flox\backslash flox}$ groups respectively, two-tailed t-test; * indicates $p<0.05$, ** indicates $p<0.01$, *** indicates $p<0.001$). For detailed statistical information, see Table 3-Source Data1.

Fig 4. Antisense-mediated MYRF knockdown in the ACC impairs memory consolidation. (A) Rats were bilaterally injected in the ACC with either scrambled (SCR, *n* = 7) or antisense oligonucleotides against Myrf (ASO, *n* = 6) 15 minutes before training and euthanized one hour (1H) later for RT-qPCR analysis of myrf mRNA levels. (B) Immunohistochemistry representative images and quantification of MBP. Rats were bilaterally injected with either SCR (*n* = 6) or AS (*n* = 4) 15 minutes before and 6 hours after training and perfused one day after training for immunohistochemistry against MBP (scale bars: 160 μm). (C, D, E) Mean latency of rats in which ACC (C, D) and dHC (E) were bilaterally injected with either scramble sequences or myrf antisense oligonucleotides. (C) Injections were given 15 minutes before training and rats were tested at one hour post-training (*n* = 6 per group) or (D) injections were given 15 minutes before and 6 hours after training and rats were tested one day, and 28 days after training *(n* = 7 per group). Rats received a reminder shock (RS) after the last testing, followed by another retention

test a day later (RS test). On day later the rats underwent re-training (RT), and memory retention was tested a day later (RT test). (E) Injections were given 15 minutes before and 6 hours after training and rats were tested one day and 28 days after training *(n* = 6 per group). Data are presented as mean latency ± s.e.m. to enter the dark chamber (in seconds, s; two-way ANOVA followed by Bonferroni *post hoc* test; * indicates P < 0.05, ** indicates P < 0.01, *** indicates P < 0.001). For detailed statistical information, see table 4-source data1.

Fig 5. Myrf knockout in the mouse ACC impairs memory formation. (A) Experimental design: AAV-MBP-CreER^{T2} was injected bilaterally into the ACC of Myrf$^{+\backslash+}$ (*n* = 3) and Myrf$^{flox\backslash flox}$ mice (*n* =5). Fourteen days following viral injection, mice were injected intraperitoneally (i.p.) with tamoxifen (TAM) every other day for 4 times, terminating seven days before the training. Mice were then injected i.p. with EdU, immediately after IA training and perfused for immunohistochemistry one day after training. (B) Diffusion of injection shown by Chicago sky blue diffusion targeted mainly the ACC (right panel). Left panel image adapted from mouse brain atlas (scale bar: 200 μm). (C) Representative immunohistochemical staining (scale bar: 40 μm) and quantification of ACC triple immunostaining of EdU, Olig2 and CC1. For each mouse, three coronal sections were quantified and averaged. In each coronal section the entire ACC was quantified bilaterally. Each dot represents the average of the three coronal sections of each mouse. Data are presented as mean percentage ± s.e.m. of positive cell number relative to Dapi+ nuclei in the ACC (two-tailed t-test). (D, E, F) mean latency to enter the dark chamber (in seconds, s). (D) AAV-MBP-CreERT2 was injected bilaterally into the ACC of Myrf$^{+\backslash+}$, and Myrf$^{flox\backslash flox}$ mice. Fourteen days following viral injection, mice were received 4 injections of (TAM) (once every other day) and seven days later they underwent IA training and were tested at one hour (1H) after training to test short-term memory (*n* = 7 per group). (E) The mice underwent the same protocol described in D but were tested at one day (1D) and seven days (7D) after training to assess for long-term memory (*n* = 7,11 per Myrf$^{+\backslash+}$, and Myrf$^{flox\backslash flox}$ groups respectively). Data are represented as mean latency ± s.e.m. two-way ANOVA followed by Bonferroni *post hoc* test. (F) AAV-MBP-CreER^{T2} was injected bilaterally into

924 the dHC of Myrf$^{+\backslash+}$ (*n* = 6) and Myrf$^{flox\backslash flox}$ mice (*n* = 7). Fourteen days following viral injection, the mice
925 received the 4 times TAM protocol and 7 days later were trained in IA. They were then tested at 1D and
926 7D after training. Data are represented as mean latency ±s.e.m. (in seconds, s; two-way ANOVA followed
927 by Bonferroni *post hoc* test, * Indicates p<0.05, *** indicates p<0.001). For detailed statistical
928 information, see table 5-source data1.
929
930 **Fig 6. Neuronal activity inhibition during learning impairs learning-induced oligodendrogenesis**
931 **and long-term memory formation.** (A) ACC targeting of viral injections. Upper panel: AAV-hSyn-
932 hM4D(Gi)-mCherry was injected stereotactically targeting the ACC of mice; the infection targeted
933 largely the ACC as shown by the mCherry expression. Lower panel; image adapted from mouse brain
934 atlas (scale bar: 200 μm). (B) Experimental and mean latency of mice injected with either C21 or Vehicle
935 (*n* = 7 per group) fourteen days following viral injection, at one hour before training. The mice were
936 tested one day (1D) following training. Data are represented as mean latency ± s.e.m. to enter the dark
937 chamber (in seconds, s; two-tailed t-test; * Indicates p<0.05). (C) ACC oligodendrogenesis assessed by
938 double staining of EdU and Olig2 in mice injected with AAV-hSyn-hM4D(Gi)-mCherry and two weeks
939 later injected i.p. with Veh or C21 one hour before training. Left: high magnification representative image
940 (scale bar: 40 μm) and Right: quantification of ACC double staining. For each mouse, three coronal
941 sections were quantified and averaged. In each coronal section the entire ACC was quantified bilaterally.
942 Each dot represents the average of the three coronal sections of each mouse. Data are presented as mean
943 percentage ± s.e.m. number of double positive cells relative to Dapi+ nuclei in the ACC (n = 3 mice per
944 group, two-tailed t-test; * Indicates p<0.05). For detailed statistical information, see table 6-source data1.
945
946 **Supplementary data Figure 1.** (A) quantifications of EdU, Olig2 and CC1 triple staining in the dHC
947 subregions CA1, CA2, CA3, and DG. Three coronal sections were quantified and averaged. In each
948 coronal section the entire CA1, CA2, CA3, or DG were quantified bilaterally. Each dot in the graphs
949 represents the average values of the three coronal section of each mouse. Data are presented as mean

950 percentage ± s.e.m. of positive cell number relative to Dapi+ nuclei (n = 4 mice per group, two-tailed t-

951 test). For detailed statistical information, see table 2-source data1.

952

953

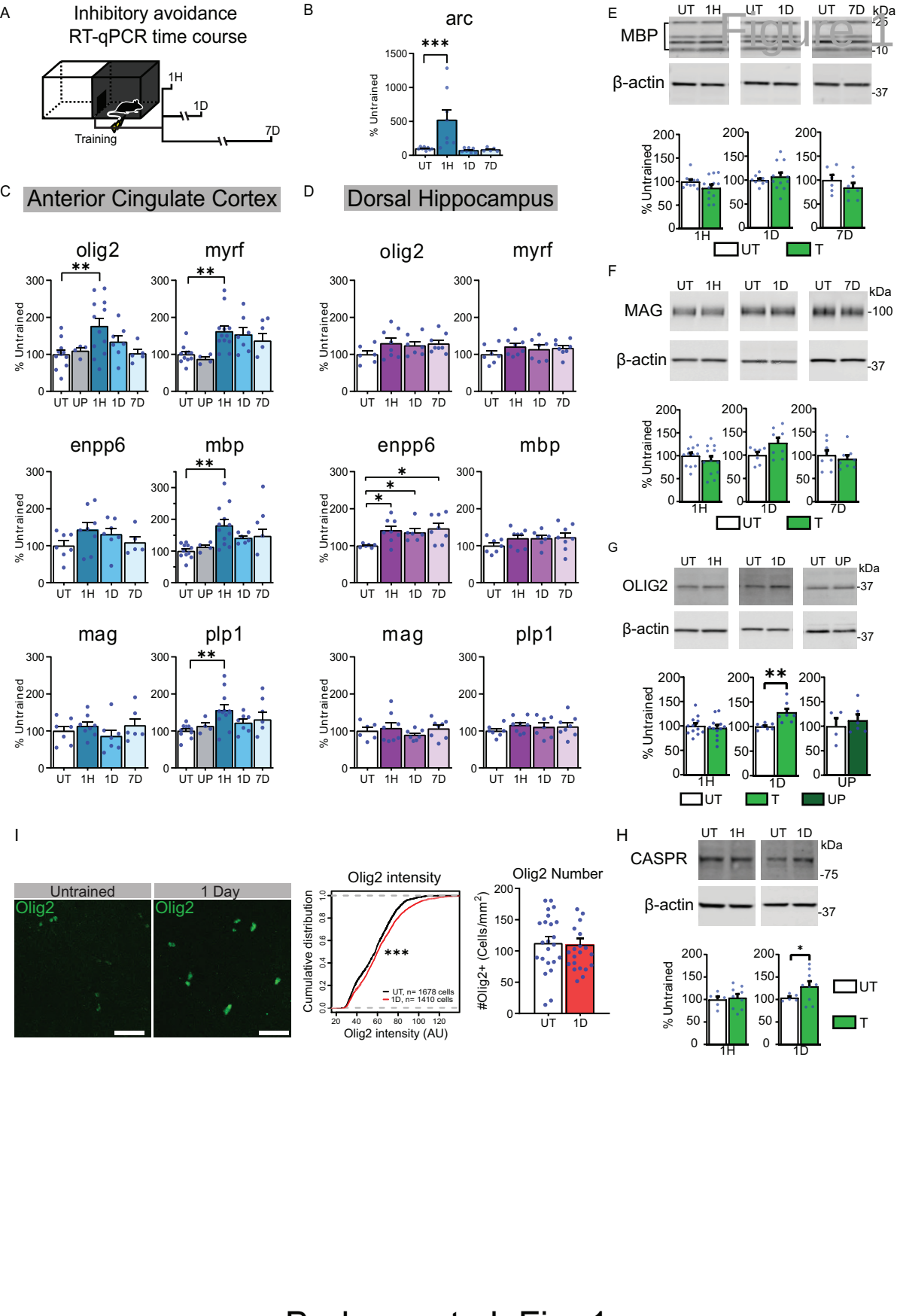

Barboza et al. Fig. 1

A

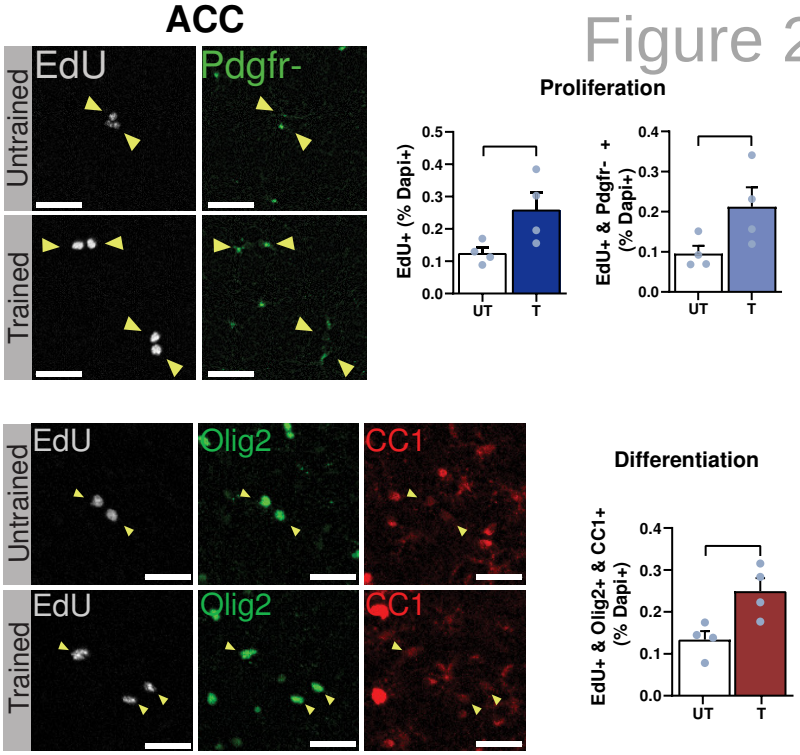
ACC
EdU
Pdgfr-
Untrained
Trained
Proliferation
EdU+ (% Dapi+)
EdU+ & Pdgfr- + (% Dapi+)
UT
T
Olig2
CC1
Differentiation
EdU+ & Olig2+ & CC1+ (% Dapi+)

B

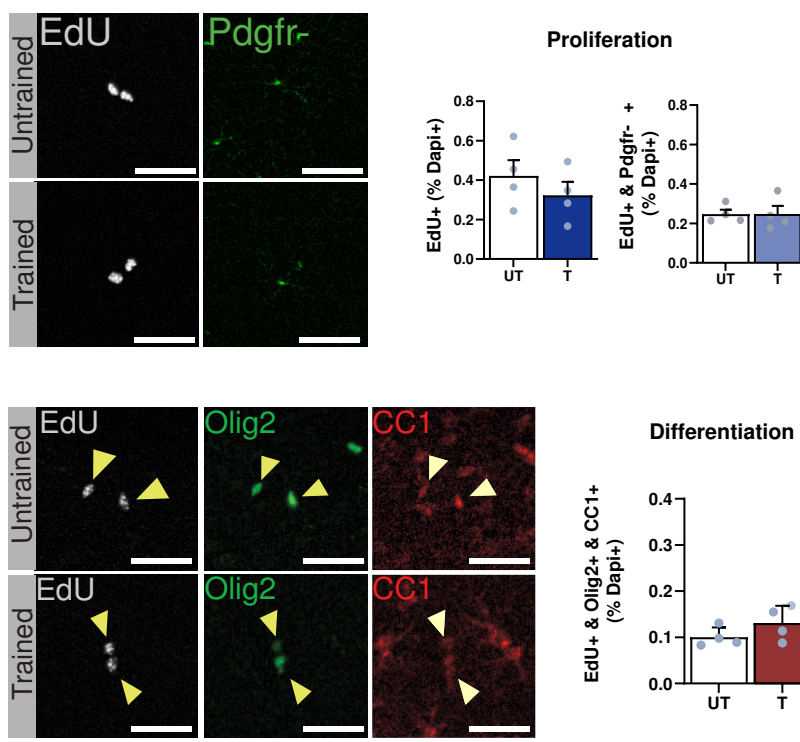
Dorsal Hippocampus
EdU
Pdgfr-
Untrained
Trained
Proliferation
EdU+ (% Dapi+)
EdU+ & Pdgfr- + (% Dapi+)
UT
T
Olig2
CC1
Differentiation
EdU+ & Olig2+ & CC1+ (% Dapi+)

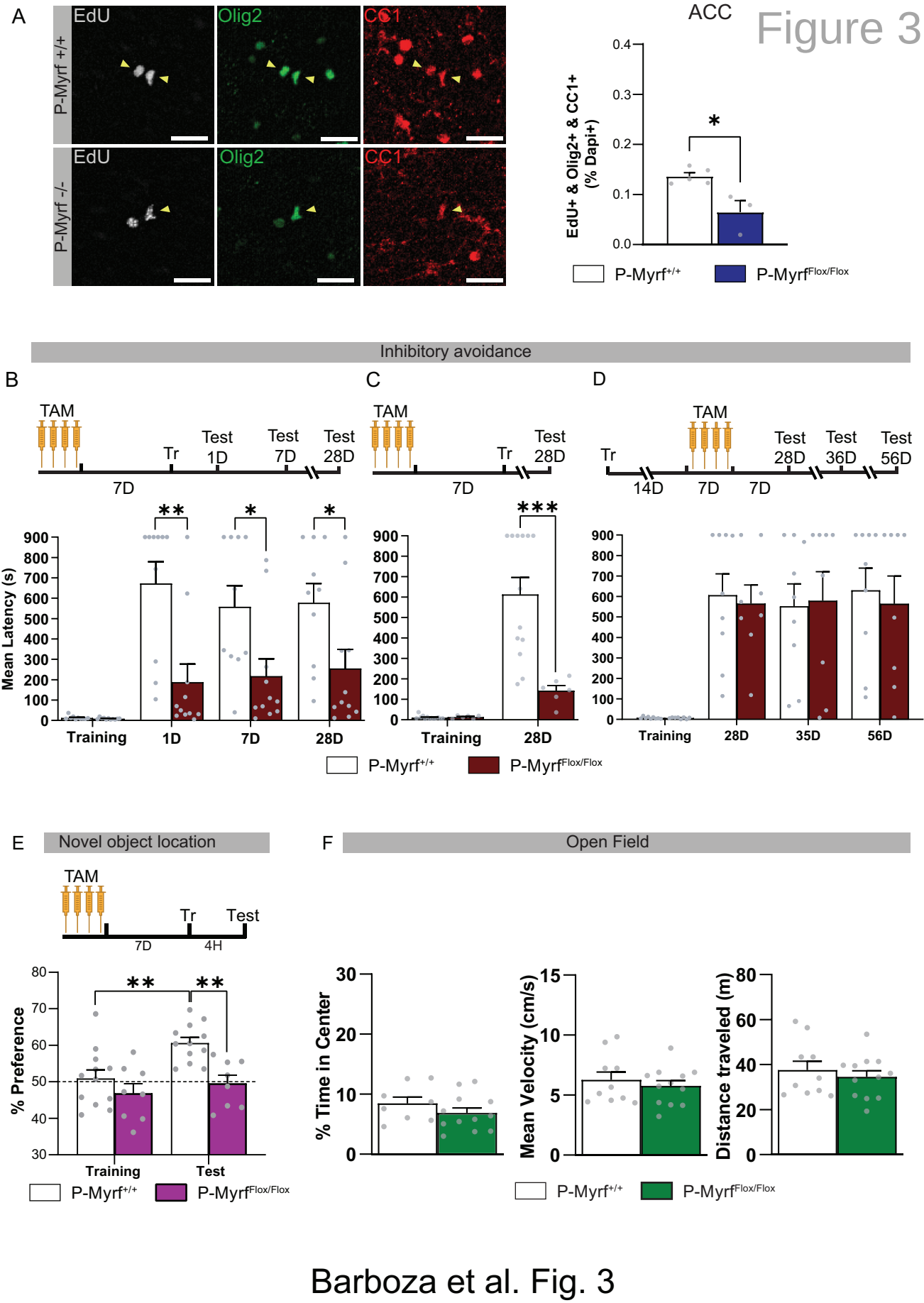

Barboza et al. Fig. 3

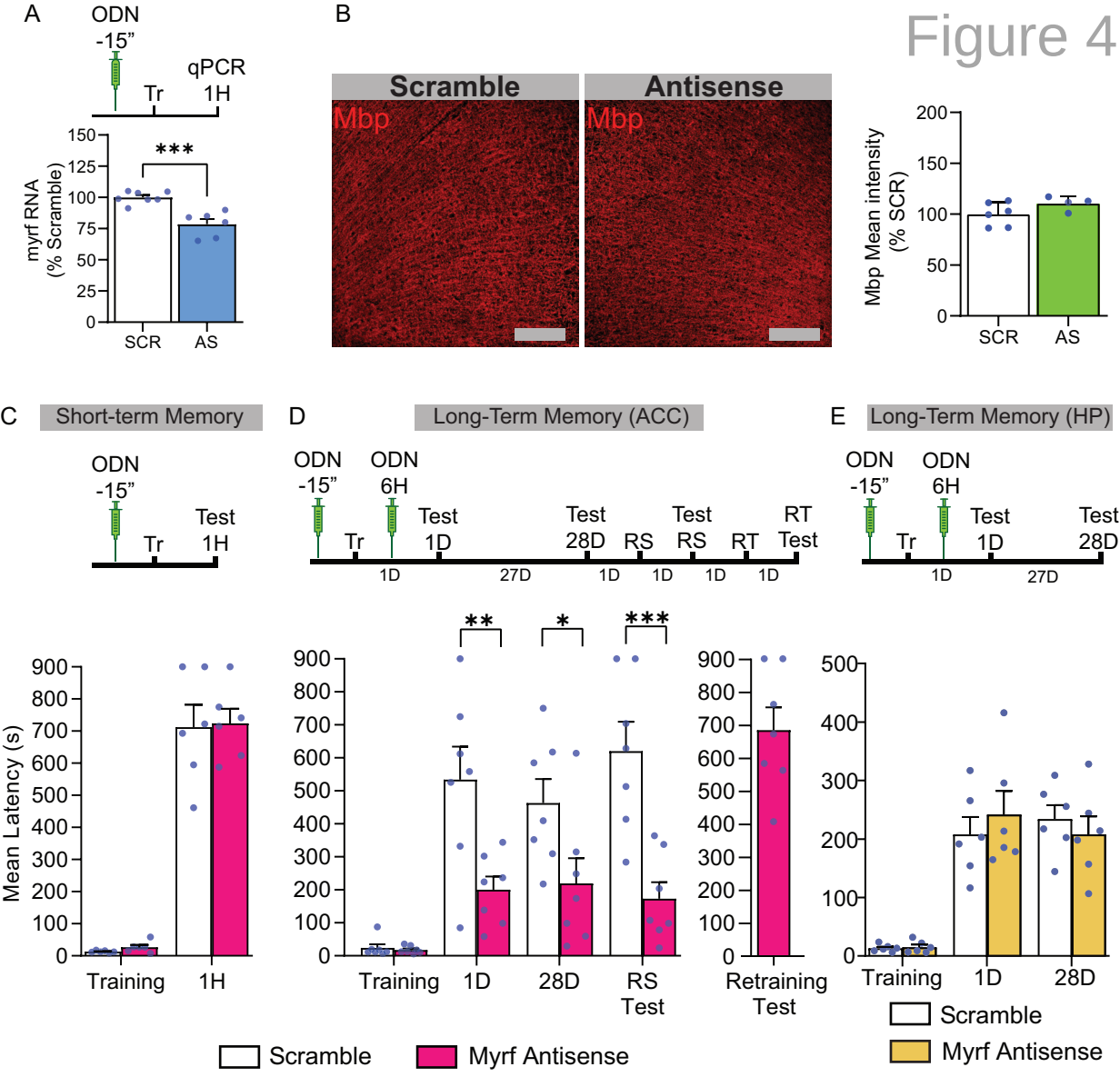
A
ODN
-15”
Tr
qPCR
1H
myrf RNA
(% Scramble)
***
SCR
AS
B
Scramble
Antisense
Mbp
Mbp
Mbp Mean intensity
(% SCR)
SCR
AS
C
Short-term Memory
ODN
-15”
Tr
Test
1H
D
Long-Term Memory (ACC)
ODN
-15”
ODN
6H
Tr
Test
1D
Test
28D
RS
Test
RS
RT
RT
Test
1D
27D
1D
1D
1D
1D
E
Long-Term Memory (HP)
ODN
-15”
ODN
6H
Tr
Test
1D
Test
28D
1D
27D
Mean Latency (s)
**
*
***
Training
1H
Training
1D
28D
RS
Test
Retraining
Test
Training
1D
28D
Scramble
Myrf Antisense
Scramble
Myrf Antisense

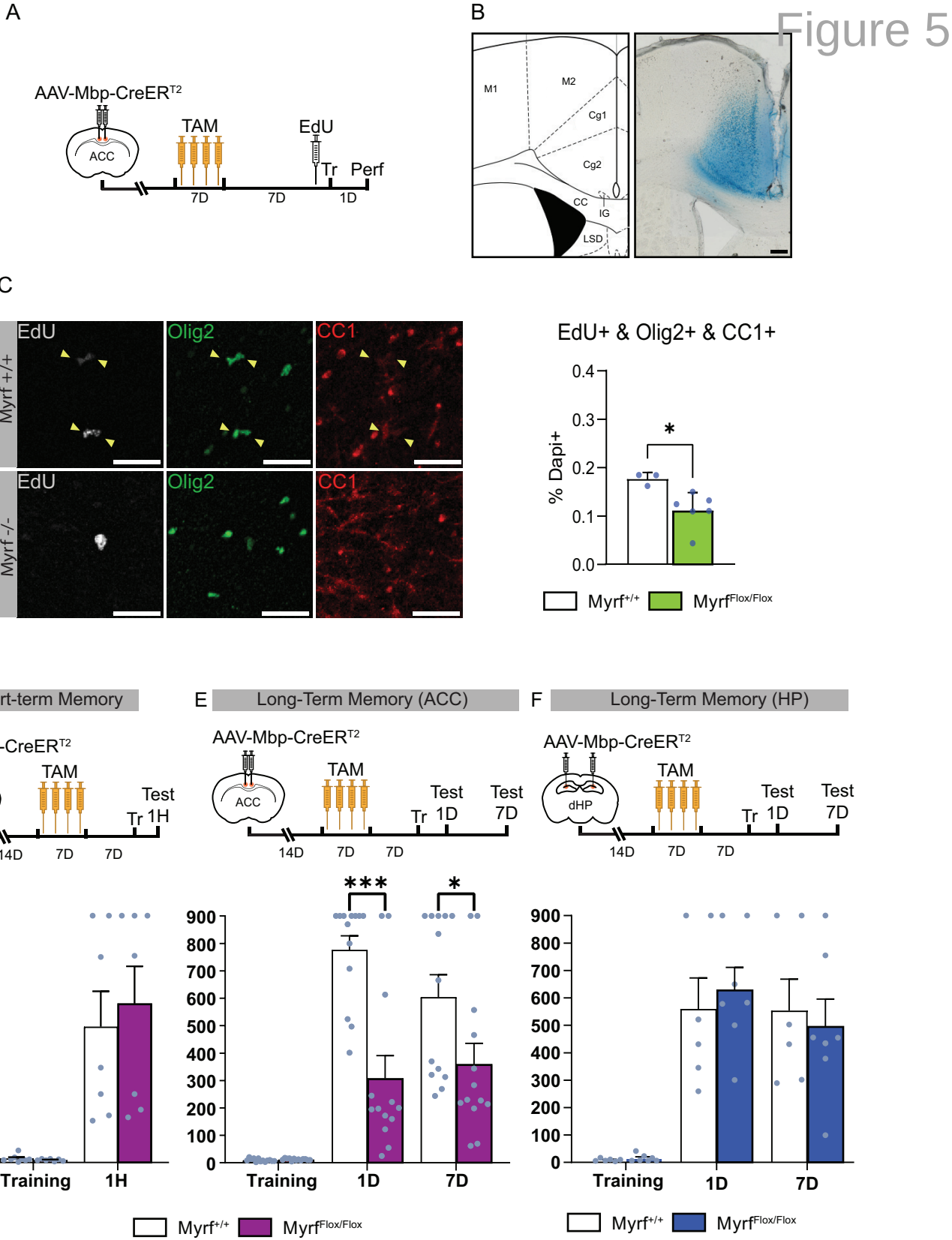

Barboza et al. Fig. 5

A

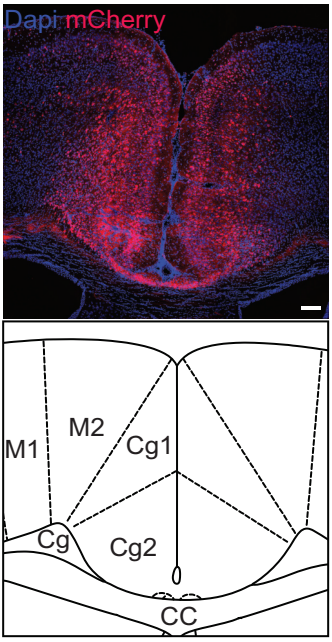
Dapi mCherry
M1
M2
Cg1
Cg
Cg2
CC

B

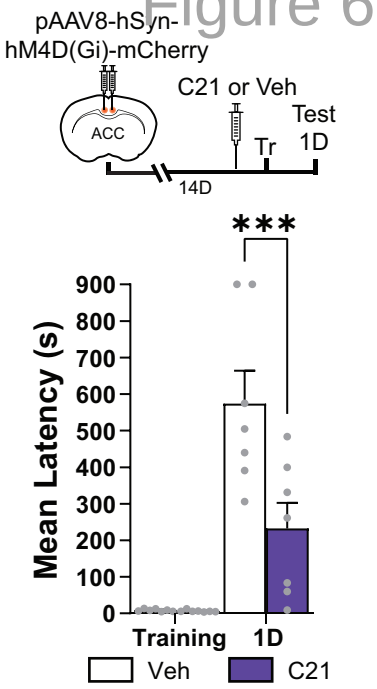
pAAV8-hSyn-
hM4D(Gi)-mCherry
ACC
C21 or Veh
Tr
Test
1D
14D
***
Mean Latency (s)
900
800
700
600
500
400
300
200
100
0
Training
1D
Veh
C21

C

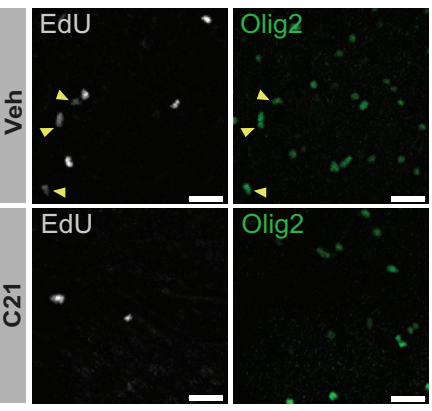
Veh
C21
EdU
Olig2
EdU
Olig2

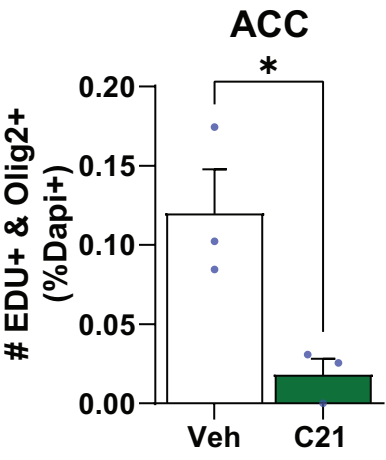
ACC
*
EDU+ & Olig2+
(%Dapi+)
0.20
0.15
0.10
0.05
0.00
Veh
C21

A

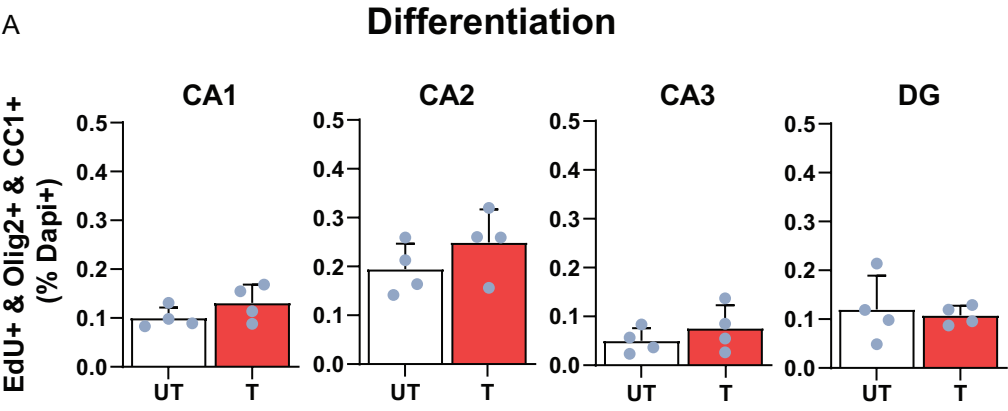

Barboza et al. Supplementary Data Fig. 1